Research Article

Arun Kumar, Sumit Chakravarthy, and Aziz Nanthaamornphong*

# Application of IoT network for marine wildlife surveillance

https://doi.org/10.1515/phys-2023-0160
received September 06, 2023; accepted November 27, 2023

**Abstract:** Every day of the week, wireless communication is almost all around us. The Internet of Things (IoT) is a standard protocol used to describe the rapidly advancing technology in which almost every electronic device is or may be connected to the Internet. These electronic gadgets constantly provide data signals to the gateways, which satellites such as those in Low Earth Orbit may transmit. Because of these networks' limited resources and the IoT, these transactions must be completed with the least amount of latency and data loss possible. We also analyze the performance implications of implementing RF-based powering for such a network. The techniques presented in this paper may benefit the scientific community and industry in general when it comes to the dynamic distributed parameter allocation methodology for IoT network devices. We will also discuss how research on animals and the natural environment has been impacted by IoT breakthroughs, in particular, animal sensors' limits and incapacity to broadcast from everywhere. Our analysis illustrates the most effective data transmission technique and establishes the bounds of these restrictions. Furthermore, the physics of the RF channel plays a critical role in the uncertainty of the channel as well as the amount of energy harvested. By employing simulation based on the physics of the RF channel, the article shows the performance of the system considering both the uncertainty of data arrival as well as the variability of the channel. The findings of the simulation show that the devices consume less energy overall as the signal-to-noise ratio rises. Furthermore, a timing factor of 10–15% is shown to be effective in maintaining a constant mean rate and increasing the energy efficiency of the system.

**Keywords:** Internet of Things, marine wildlife, wireless communication

## 1 Introduction

Our civilization is changing quickly and continuously; thus, it is crucial for technology to advance with little lag. Wi-Fi 6, 5G and 6G wireless networks, and Vehicle-to-Everything Wireless are examples of emerging technological standards that depend on wireless communication and architecture designed for the Internet of Things (IoT). Not only has technology altered how we go to the doctor or do our schoolwork, but it has also aided in the greater understanding and global tracking of animals and other creatures by scientists [1]. The Internet of Wildlife and Animals is shedding new light on a number of previously unexplained or unreported phenomena, including why whales return to certain oceans once a year, why sharks move thousands of kilometres every year to isolated locations, and many others. The sensors fitted to animals that can follow their movements and behaviours while sending important data to surrounding sensors, buoys, and gateways enable this tracking technique [2]. A variety of satellite orbit architectures have been developed in relation to satellite communication technologies to support the development of IoT. These collections of interconnected satellites constitute satellite constellations that assist in offering coverage in almost every region of the world [3]. Satellites in geosynchronous equatorial orbits, or GEOs, are the farthest from the planet and typically orbit in a direction perpendicular to their spin. In general, GEO satellites orbit the Earth for a whole day and are a little more than 20,000 miles from the surface. The Medium Earth Orbit satellite is another one that revolves around the planet. In comparison to GEO satellites, these spacecraft orbit at a significantly lower altitude, typically between 3,000 and 8,000 miles above the planet [4]. When compared to GEO satellites, the satellites' close proximity to the Earth's surface

* **Corresponding author: Aziz Nanthaamornphong**, College of Computing, Prince of Songkla University, Phuket, Thailand, e-mail: aziz.n@phuket.psu.ac.th
**Arun Kumar:** Department of Electronics and Communication Engineering, New Horizon College of Engineering, Bengaluru, India, e-mail: dr.arunk.nhce@newhorizonindia.edu
**Sumit Chakravarthy:** Department of Electrical Engineering and Computer Engineering, Kennesaw State University, Kennesaw, GA, United States of America, e-mail: schakra2@kennesaw.edu

significantly lowers communication latency. It has been observed that these satellites orbit the Earth in 5 h, give or take 3 h. More than 1.5 gigabits of data may be sent per second using GEO satellites [5]. However, Low Earth Orbit (LEO) satellites are the ones that have recently drawn the greatest interest. Many billionaires and private businesses are vying for the top spot in creating technologies that will allow us to use these satellites most effectively on a daily basis. LEO satellites orbit the planet at a height of little more than 1,000 ft. These satellites are the best option for constructing quick communication lines with low latency due to their location [6]. The shift and race to establish wireless communication using LEO satellites is driven by the need to reduce latency, reduce signal distortion, and increase dependability. The monitoring of animals in the water and on land has been the subject of several programmes and studies. The International Cooperation for Animal Research Using Space initiative is one of the most significant of these initiatives. A multinational group of scientists are working on this research under the direction of Martin Wikelski. The objective of the research is to increase knowledge about how animals interact with one another and their surroundings on Earth [7]. The tracking equipment was placed on the International Space Station in the summer of 2018 to assist with this effort. Although the notion of employing satellites is not new, this thesis seeks to develop it by providing techniques to increase the model's effectiveness [8]. RF channels propagate electromagnetic waves, particularly in the radio frequency spectrum. Wireless communication systems require an understanding of the physics of RF channels. RF channel physics can be summarized as follows: Transmission of electromagnetic waves occurs over RF channels, which propagate through free space or other media. Wave propagation physics, including concepts like wavelength, frequency, and wave polarization, play an important role. Signal strength is reduced as electromagnetic waves travel through a medium. Losses are determined by factors such as distance, obstacles, and environmental characteristics [9]. A signal with multiple paths to reach the receiver is called multipath fading; this causes both constructive and destructive interference. This phenomenon in RF channel physics affects the quality of communication links. Electromagnetic waves reflect when they bounce off surfaces, refract when they pass through different media, and diffract when they bend around obstacles. These phenomena complicate RF channel physics. When waves travel through a medium, they undergo a Doppler shift due to relative motion between transmitter and receiver. Communications systems on mobile devices are particularly affected by this. Wireless communication systems, such as Wi-Fi, cellular networks, and other wireless technologies, require an understanding of RF channel physics. We consider these factors when designing the simulation of the RF communication and energy harvesting aspects to make our paper consider these physical phenomena [10]. The article is organized in the following manner: Section 1 includes an introduction, motivation, and purpose of the proposed article, Section 2 represents related work, Section 3 is the system model, and Sections 4 and 5 represent the simulation results and conclusion.

## 1.1 Motivation

- The application of the IoT network for marine wildlife surveillance is a compelling endeavor that combines cutting-edge technology with environmental conservation. It offers the opportunity to protect and monitor fragile marine ecosystems, safeguard endangered species, and contribute to scientific research. The sense of purpose in preserving our oceans and the planet's biodiversity is a powerful motivator. Additionally, the challenge of developing innovative solutions in a dynamic and complex marine environment is intellectually stimulating [11]. By working on this article, one can make a meaningful difference in the world while pushing the boundaries of IoT technology, making it a deeply rewarding and exciting pursuit.
- Collaborating between science and technology is not a new idea. Working together for decades, the specialists in these two fields have produced outcomes that have improved society's quality of life and saved lives. Developing, examining, and demonstrating methods for optimizing power and energy parameters while employing LEO satellites to monitor marine life is the aim of this project. We shall utilize a two-tiered model to illustrate our idea. Several factors will be considered by our formulas in order to help generate a more accurate optimization outcome [12]. Unlike most previous works that focused on monitoring without taking into account the size, functionality, and energy usage of the IoT sensor and network, we optimize these criteria while keeping in mind channel medium constraints, energy harvesting constraints, and especially sensor data transmission integrity. Our protocol ensures that statistical sensor data loss is minimized while optimizing IoT transmission power in a distributed manner, despite constraints on the size of the queue (buffer) for IoT equipment and the transmission channel [13].

### 1.2 Purpose of this study

The oceans store around 96.5% of the water on Earth, which covers about 71% of its surface. The ocean serves as the foundation for all life on Earth and as the core of the climate. It transfers warm water from the tropics to colder regions and cool water from the poles to warmer regions by absorbing the majority of the heat from the sun. In doing so, the ocean disperses heat and evens out the unequal distribution of solar energy that strikes Earth. Temperatures at the poles would be considerably lower, and temperatures in the tropics would be substantially higher without the currents that circulate the warm and cold seas [14]. The use of fossil fuels like natural gas, oil, and coal has boosted atmospheric carbon dioxide levels by 30% since 1950, which has led to an average temperature increase of 1.4°F throughout the course of the twentieth century. The warming of the atmosphere, land, and seas is brought on by the rise in carbon dioxide, which acts as a blanket to trap the heat of the planet. Global warming is the term for this. Even though 1.4 degrees may not seem like much, picture your body temperature rising by that amount. It would feel like the start of a fever. For our planet, nothing is different. Similar to how humans favour certain temperature ranges, many marine species do as well [15]. The majority of marine creatures have demonstrated the ability to adapt to the increasing ocean water temperatures, but the food that seals, whales, dolphins, and other species depend on is shifting owing to the warming water. Because they are diving farther and deeper into the ocean in search of cooler water, sea lions are having difficulty locating their favorite fish, sardines, and anchovies [16]. As a result of the greater distance, sea lions must use more energy when hunting and traveling. In recent years, California has seen record-high water temperatures, which has led to thousands of ill sea lions washing up on the shore after their moms abandoned their young because they had to go farther and go food hunting. Dolphin calves can't hunt for food as deeply or as far, which makes them unwell and unable to protect themselves. Our goal is to increase the availability and effectiveness of animal tracking using satellite tags for marine species. Having the capacity to follow smaller creatures like sardines and anchovies enables us to understand where they travel despite climatic change, which in turn enables us to understand how and why animals move along the same migration patterns as them for feeding, such as sea lions, dolphins, and sharks. We may discover the animal's preferred habitats, breeding sites, and nursery grounds by employing the trackers. Due to climate change and the warming of the oceans, everything is constantly changing.

## 2 Related work

In this section, we have described the related articles published so far in scientific journals. It will make it easier for readers to compare the work with earlier works and comprehend the context of the suggested study problem. The ABCOA, flower pollination algorithm, firefly algorithm, Krill herd algorithm, and genetic optimization algorithms were tested on soil temperature, pest detection, aerial pesticide and fertilizer spraying, water reservoir management, renewable power integration, and path planning for agricultural machinery. The results showed that the BIAs can be useful in new ways. Because the bio-inspired ANN algorithms used neural networks to simulate brain functions, they performed better. On the other hand, the GA algorithms were chosen due to their superior performance in several applications such as machinery path optimization, pesticide application, and crop planning models [17]. The rigorous appraisal of scholarly research concerning IoT in agriculture demonstrated that emerging technologies such as artificial intelligence sensors, actuators, uncrewed aerial vehicles, satellites, big data analytics, intelligent machines, and radio-frequency identification devices had multiple and practical areas of application in smart greenhouses and precision agriculture. Theoretical evidence shows the progress made in research and development coupled with would catalyze the uptake of these technologies. Commercial farms have demonstrated that it was practical to improve crop yield and monitor growth conditions (temperature, humidity, and nutritional content) [18]. Concern over climate change has led to an increase in interest in marine environmental monitoring. In the last few decades, numerous maritime environmental monitoring systems have been developed using cutting-edge information and communication technology. The IoT is one tool that has proved crucial in this field. An overview of the use of IoT in the realm of maritime environment monitoring is provided in this study. A brief overview of new technologies, such as sophisticated big data analytics, and their uses in this field is given. It also covers important research prospects and difficulties in this field, such as the possible use of big data and the IoT in the preservation of maritime environments [19]. This study presents a thorough analysis of the most recent studies that have been applied to the field of smart water pollution monitoring systems. The study suggests an affordable and effective IoT-based smart water quality monitoring system that continuously analyzes the quality parameters. Three water samples are used to evaluate the constructed model, and the parameters are sent to the cloud server for additional processing [20]. The proposed system in this work is

made up of multiple sensors that detect different characteristics, such as the surrounding atmosphere's temperature and humidity, the level of water in the tank, the turbidity of the water, and the pH value. Additionally, these sensors were interfaced with the Microcontroller Unit, and additional processing was carried out on a personal computer. To monitor the water quality, the ThinkSpeak program, which is based on the IoT, sends the collected data to the cloud [21]. This viewpoint article outlines some of the difficulties in conducting long-term coastal observations and offers suggestions for filling in current gaps. We go over how cooperative robotics between unmanned platforms plays a part in coastal regions and how to take advantage of IoT technologies [22]. This project's main objective is to design and construct a wireless sensor network system that will monitor bodies of water in order to save underwater life. The primary cause of pollution in aquatic environments is an overabundance of nitrogen and phosphorus, which lowers oxygen levels and poses a serious threat to marine life, including whales, sharks, and penguins. Monitoring pollution is crucial to the preservation of marine life. It is concluded that this technique is very helpful for fish production and meeting future food demands if the right management of rivers and ponds is completed with its assistance [23]. A multitude of intelligent gadgets that can communicate with one another are connected through the IoT with the least amount of human intervention possible. IoT is quickly taking up in computer science fields. The cross-cutting design of the diverse components and IoT systems involved in implementing such schemes, however, presents significant security challenges. The use of security protocols, such as application security, authentication, encryption, and access networks, for IoT systems and their fundamental security flaws is ineffective. Using earlier research on DL and ML, the authors attempted to create a review of IoT dangers while researching machine learning privacy and security concerns. There is a discussion of fresh problems and ideas from ML and DL in IoT security. In addition, recommendations for enhancing future technology are given, along with security issues, constraints, and future directions [24]. This study investigates the difficulties and limitations that arise when the IoT serves as the foundation for an over-the-horizon (OTH) marine surveillance system. The communication infrastructure of the service, which is based on high-frequency surface wave radars, is a satellite communication network in hostile settings. Currently, the entire IoT OTH maritime surveillance network is situated in the Gulf of Guinea, an unsuitable location for sensors and communications because of its tropical climate. The authors of this study have looked at how well the Gulf of Guinea's services work in a variety of weather scenarios [25].

## 2.1 System model

The system model for the study being presented is shown in Figure 1. Although it hasn't been practiced for a very

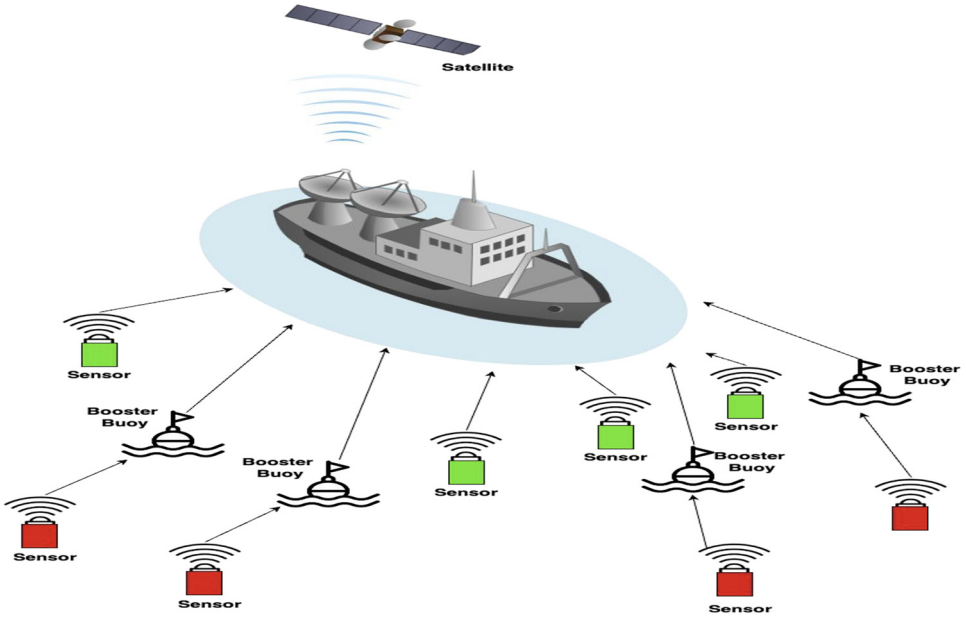


**Figure 1:** System model.

long time, animal tracking has advanced significantly in recent years. In 1804, John Audubon adorned the birds in a nest not far from his house with silver threads. One of the earliest tests with "animal tracking" was carried out the following spring when two of them returned with the line still attached. Now that we have sensors that attach to animals, we can follow their movements and determine why they move in particular ways using GPS and satellite technology [26]. They used LEO tags to follow the individual manta rays in earlier research, similar to the Manta Matcher trackers. The tag is set to expire after six months. Then, in order to receive their data, the scientists must wait for the tracker to wash ashore. The data are lost if the tracker is lost at sea. In order to keep up with the manta rays they are monitoring, they also memories their markings. The ability to follow manta rays is a terrific idea because they are now listed as an endangered species owing to climate change and poachers who go after them for Chinese medicine. This thesis explains why it's important for us to be able to monitor an ecosystem that includes all varieties of marine life, including creatures like the manta ray [27]. Our sensors are unique because we are embedding them into the Great Barrier Reef. We can readily get them by boat, so they won't need to wash ashore and remain immobile. Additionally, we have set the sensors up to download data to the gateway automatically.

In case the sensor requires assistance sending the data to the gateway depicted in Figure 2a and b, we have additionally put booster buoys. With the sensors being stationary inside, the ecosystem we will not only be able to monitor the ecosystem but also the habitat of many of the marine life in the Great Barrier Reef.

$M + N$, where $N$ is the number of direct IoT uplinks and $M$ is the number of IoT uplinks through boosters, is the total number of slots available to transmit in a frame at the gateway. The boosters synchronize the two-time frames by making $M + N$ the total time slots as well. The neighborhood IoTs will use N-A only to relay data to the booster. Finally, the $M$ time slots are utilized for the actual transfer of the IoT data *via* the booster after A time slots are set aside for the Booster to prioritize its data transfer. In Figure 2, the two-tier approach that we will be employing is depicted. There are a total of $K$ sensor devices that can broadcast data to the gateway directly, along with $W$ booster buoys. Only $N$ devices, chosen from a possible list of $K$, IoT sensors, and $M$ devices, corresponding indirect transmission *via* the $W$, Boosters by potentially $L$, IoT-based sensors, may be scheduled to transmit at a period. A transmission time of $T/(N + M + 1)$ will be given to the transmitting devices $N$ and $M$ since the 1 slot is set aside for the scheduling decision. Figure 2 illustrates how the remaining slots will be used for data transfer. A test signal will be transmitted from the gateway to the sensors to ascertain the signal strength corresponding to the channel, where i can either correlate to the IoTs or the Boosters, before the connection begins. A similar setup is also taken into account for the booster. For sensors that can communicate directly to the gateway, the upper $M$ slots will be set aside. During this time period, sensors with weak signals will be sent to the booster buoy. To allow for transmission from these booster buoys, $N$ slots will be set aside. The neighborhood IoTs can transmit signals to the booster buoys. It is thought that sending the full packet to the satellite after these data have been received at the gateway is outside the purview of the task. The IoT gadgets are thought to be self-sufficient. Solar energy provides them with their energy. Our gadgets' cost is not significantly increased by this energy gathering. We upgrade to take

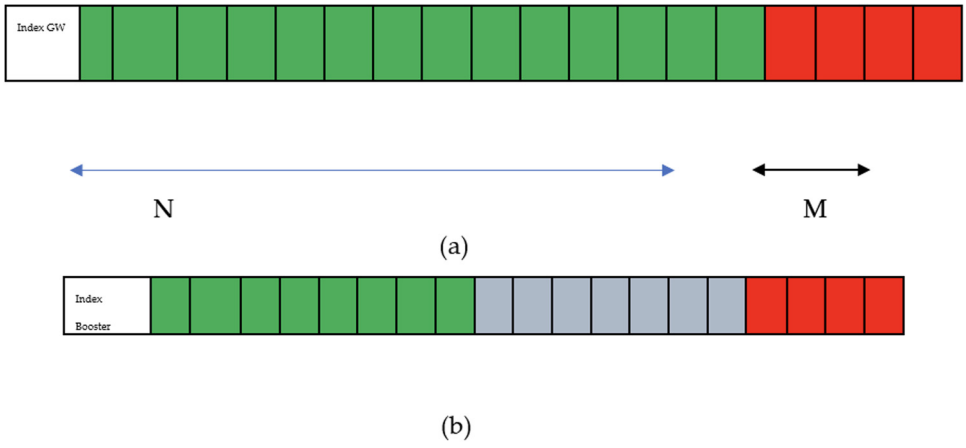


**Figure 2:** Timeslots: (a) for gateway connectivity and (b) for booster connectivity.

into account RF energy harvesting by IoT sensors in the subsequent section. We just take into account one booster buoy for the purpose of simplicity. $s_x^{[i]}$ is a binary indicator used to show whether the $x$th IoT device at the $i$th frame is scheduled for transmission. Also $[i]$ represents the frame., $x \in k, l, w = 1$, *i.e.*, either IoTs sending data direction or *via* the boosters [28].

$$s^{[i]} = \begin{cases} 0; \text{if not scheduled} \\ 1; \text{if scheduled} \end{cases}.$$

The total energy consumption will be the energy required from the sensors, booster buoys, and booster-based sensors. Energy consumption from each sensor to the gateway [29]:

$$E_{\text{total}}^{\text{sen}} = \{s_k^{[i]} p_k^{[i]}\}, \tag{1}$$

where $p_k^{[i]}$ represents the power used by the $k$th sensor. The energy consumption coming from each booster buoy can be represented as follows:

$$E_{\text{total}}^{\text{booster}} = \{s_w^{[i]} p_w^{[i]}\}\tau, \tag{2}$$

where $p_w^{[i]}$ represents the power used by the $w$th booster device. Energy consumption from each booster connected sensor to its booster [30]:

$$E_{\text{total}}^{\text{Bsen}} = \{s_l^{[i]} p_l^{[i]}\}\tau, \tag{3}$$

where $p_l^{[i]}$represents the power used by the $l$th sensor. All of the above equations apply to the $i$th time frame. Total energy consumption can be represented as [31]

$$E_{\text{total}} = E_{\text{total}}^{\text{sen}} + E_{\text{total}}^{\text{Bsen}} + E_{\text{total}}^{\text{booster}}$$

Or,

$$E_{\text{total}} = \sum_{k=1}^{K} s_k^{[i]} p_k^{[i]}\tau + \sum_{w=1}^{W} s_w^{[i]} p_w^{[i]}\tau + \sum_{l=1}^{L} s_l^{[i]} p_l^{[i]}\tau. \tag{4}$$

The total energy consumption is shown to be the summation of the energy of each of the sensors sent to either the main gateway for the $k$ devices or the booster buoys for the $w$ devices. This is added to the energy consumed by the IoT which sends data *via* the booster route. The service rate for each device to the gateway will represent the power, and the channel condition is written as follows:

$$g\{p_k^{[i]}, h_k^{[i]}\} = B \log_2[1 + p_k^{[i]} h_k^{[i]}];\ \forall k, i, \tag{5}$$

$$g\{p_w^{[i]}, h_w^{[i]}\} = B \log_2[1 + p_w^{[i]} h_w^{[i]}];\ \forall k, i, \tag{6}$$

$$g\{p_l^{[i]}, h_l^{[i]}\} = B \log_2[1 + p_l^{[i]} h_l^{[i]}];\ \forall k, i, \tag{7}$$

where $B$ is the occupied channel bandwidth standardized for the system. The queue will be continuously updated for these devices as follows:

$$Q_k^{[i+1]} = \max[Q_k^{[i]} - g\{p_k^{[i]}, h_k^{[i]}\} s_k^{[i]}\tau, 0] + \theta_k^{[i]} T. \tag{8}$$

The above represents the direct path sensor queue.

$$Q_w^{[i+1]} = \max[Q_w^{[i]} - g\{p_w^{[i]}, h_w^{[i]}\} s_w^{[i]}\tau, 0] + \sum_{l=1}^{L} \phi_l^{[i]} T. \tag{9}$$

Where,

$$\phi_l^{[i]} = g\{p_l^{[i]}, h_l^{[i]}\} s_l^{[i]}\tau, \tag{9a}$$

$$Q_l^{[i+1]} = \max[Q_k^{[i]} - g\{p_l^{[i]}, h_l^{[i]}\} s_l^{[i]}\tau, 0] + \theta_l^{[i]} T. \tag{10}$$

Eqs. (9) and (10) describe queue updates at the booster and IoTs that use the booster to send data, respectively. The following equation may be used to reduce the energy consumption problem for the sensors that can broadcast directly to the gateway, booster buoy, and gateway:

$$\min f(\{p_k^{[i]}, s_k^{[i]}\}, \{p_w^{[i]}, s_w^{[i]}\}, \{p_l^{[i]}, s_l^{[i]}\}) = \min \left[ \sum_{k=1}^{K} s_k^{[i]} p_k^{[i]}\tau + \sum_{w=1}^{W} s_w^{[i]} p_w^{[i]}\tau + \sum_{l=1}^{L} s_l^{[i]} p_l^{[i]}\tau \right]. \tag{11a}$$

Such that mean rate stability is achieved for the queues belonging directly to communication sensors, booster, and indirectly to communicating sensors. Therefore, mean rate stability applies to [32]

$$Q_k^{[i]} \quad \forall k \in K, \forall i, \tag{11b}$$

$$Q_w^{[i]} \quad \forall w \in W, \forall i, \tag{11c}$$

for the booster buoy and,

$$Q_l^{[i]} \quad \forall l \in L, \forall i, \tag{11d}$$

for the indirect communicating IoT. Furthermore, the indicator variables have the following constraints:

$$\sum_{k=1}^{K} s_k^{[i]} = N;\ \forall i, \tag{11e}$$

$$\sum_{w=1}^{W} s_w^{[i]} = M;\ \forall i, \tag{11f}$$

$$s_k^{[i]} \in \{0, 1\};\ \forall k \in K, \forall i, \tag{11g}$$

$$s_w^{[i]} \in \{0, 1\};\ \forall w \in W, \forall i, \tag{11h}$$

$$p_k^{[i]} \in \overrightarrow{P_{\text{IOT}}};\ \forall k \in K, \forall i, \tag{11i}$$

$$p_w^{[i]} \in \overrightarrow{P_{\text{BR}}};\ \forall w \in W, \forall i, \tag{11j}$$

$$p_l^{[i]} \in \overrightarrow{P_l};\ \forall l \in L, \forall i. \tag{11k}$$

The design variables for the problem above (11a) are $p_k^{[i]}, s_k^{[i]}, p_w^{[i]}, s_w^{[i]}, p_l^{[i]}, s_l^{[i]}, p^{[i]}$. Eqs. (11b)–(11d) are to maintain the sensors, booster buoy, and IoT to booster queue so that they remain stable. Eqs. (11e) and (11f) show that there are only $N$ and $M$ number of devices that are scheduled within

the timeframe. Eqs. (11g) and (11h) represent the scheduling being binary where 0 does not transmit and 1 transmits. Eqs. (11i)–(11k) correspond to the power of the IoT sensor, the booster buoy, and the power of IoT to booster.

## 2.2 Problem transformation

In this section, we will be using Lyapunov optimization on the problem in (11a). We will again split this into a subproblem representing the sensors and booster and the indirect IoT system [28].

$$\min_{\{p_k^{[i]},s_k^{[i]},p_w^{[i]},s_w^{[i]},p_l^{[i]},s_l^{[i]}\}} \left[\sum_{k=1}^{K} s_k^{[i]} p_k^{[i]}\tau \sum_{w=1}^{W} s_w^{[i]} p_w^{[i]}\tau + \sum_{l=1}^{L} s_l^{[i]} p_l^{[i]}\tau\right].$$

Operation is broken into the following two parts:

$$\min_{\{p_k^{[i]},s_k^{[i]}\}} \sum_{k\in K} s_k^{[i]} p_k^{[i]}\tau, \tag{12}$$

s.t. (11b), (11e), (11g), (11j), (11k)

$$\min_{\{p_w^{[i]},s_w^{[i]}\}} s_w^{[i]}, p_w^{[i]}\tau + \sum_{l\in L} s_l^{[i]}, p_l^{[i]}\tau, \tag{13}$$

s.t. (11c), (11f), (11h), (11j), and (11k)

The Lyapunov Function from the problem above for the close sensor, booster buoy, and gateway will be listed as follows:

$$\mathscr{L}[Q_x^{[i]}] \quad \triangleq \quad \frac{1}{2}\sum_{x\in X} (Q_x^{[i]})^2; \forall i \tag{14}$$

The Lyapunov Drift for the devices is written as follows:

$$\Delta(Q_x^{[i]}) \triangleq \mathrm{E}\{\mathscr{L}[Q_{\mathrm{x}}^{[i+1]}] \quad \mathscr{L}[Q_x^{[i]}] | \, Q_x^{[i]}\} \, \forall i, \tag{15}$$

where $x \in \{k, l, w = 1\}$ By combining Eqs. (14) and (15), we get the transformed objective for the direct IoTs asshown in (16) and (17):

$$\begin{aligned}
\Delta(\boldsymbol{Q}_K^{[i]}) &= \frac{1}{2}\sum_{k\in\mathscr{K}} \mathbb{E}\{(Q_k^{[i+1]})^2 - (Q_k^{[i]})^2 | \, \boldsymbol{Q}_K^{[i]}\} \\
&\le \frac{1}{2}\sum_{k\in\mathscr{K}} \{(Q_k^{[i]})^2 + (g\{p_k^{[i]}, h_k^{[i]}\}s_k^{[i]}\tau)^2 + (\theta_k^{[i]}T)^2 \\
&\quad - 2Q_k^{[i]}(g\{p_k^{[i]}, h_k^{[i]}\}s_k^{[i]}\tau - \theta_k^{[i]}T) \\
&\quad -2g\{p_k^{[i]}, h_k^{[i]}\}s_k^{[i]}\tau\theta_k^{[i]}T - (Q_k^{[i]})^2\} \\
&\le \sum_{kin\mathscr{K}} \frac{1}{2}(g\{p_k^{[i]}, h_k^{[i]}\}s_k^{[i]}\tau - \theta_k^{[i]}T)^2 \\
&\le \sum_{k\in\mathscr{K}} \left\{\frac{1}{2}(g\{p_k^{[i]}, h_k^{[i]}\}.^{[i]}_k\tau - \theta_k^{[i]}T)^2 \right. \\
&\quad \left. + Q_k^{[i]}(\theta_k^{[i]}T - g\{p_k^{[i]}, h_k^{[i]}\}s_k^{[i]}\tau)\right\} \\
&\le \sum_{k\in\mathscr{K}} \{Q_k^{[i]}(\theta_k^{[i]}T - g\{p_k^{[i]}, h_k^{[i]}\}s_k^{[i]}\tau)\}
\end{aligned} \tag{16}$$

$$\begin{aligned}
\Delta(\boldsymbol{Q}_W^{[i]}) &= \frac{1}{2}\mathbb{E}\{(Q_w^{[i+1]})^2 - (Q_w^{[i]})^2 | \, \boldsymbol{Q}_W^{[i]}\} \\
&\le \frac{1}{2}\{(Q_w^{[i]})^2 + (g\{p_w^{[i]}, h_w^{[i]}\}s_w^{[i]}\tau)^2 + \sum(\theta_l^{[i]}T)^2 \\
&\quad - 2Q_w^{[i]}(g\{p_w^{[i]}, h_w^{[i]}\}s_w^{[i]}\tau - \sum\theta_l^{[i]}T) \\
&\quad -2g\{p_w^{[i]}, h_w^{[i]}\}s_w^{[i]}\tau\theta_l^{[i]}T - (Q_w^{[i]})^2\} \\
&\le \sum_{w\in W} \frac{1}{2}(g\{p_w^{[i]}, h_w^{[i]}\}s_w^{[i]}\tau - \sum\theta_l^{[i]}T)^2 \\
&\le \sum_{w\in W} \left\{\frac{1}{2}(g\{p_w^{[i]}, h_w^{[i]}\}s_w^{[i]}\tau - \sum\theta_l^{[i]}T)^2 + Q_w^{[i]}(\sum\theta_l^{[i]}T \right. \\
&\quad \left. - g\{p_w^{[i]}, h_w^{[i]}\}s_w^{[i]}\tau)\right\} \\
&\le \sum_{w\in W} \{Q_w^{[i]}(\sum\theta_l^{[i]}T - g\{p_w^{[i]}, h_w^{[i]}\}s_w^{[i]}\tau)\} \\
&= \left\{Q_w^{[i]}\left[\sum_{l}^{L}(g\{p_l^{[i]}, h_l^{[i]}\}s_l^{[i]}\tau) - g\{p_w^{[i]}, h_w^{[i]}\}s_w^{[i]}\tau\right]\right\}
\end{aligned} \tag{17}$$

So, finally, the Lyapunov drift and penalty representation can be written as follows:

$$\begin{aligned}
\widetilde{F_K}(\{p_k^{[i]}, s_k^{[i]}\}) &= \Delta(Q_x^{[i]}) + V_K\sum_{k\in K} s_k^{[i]}p_k^{[i]}\tau \\
&\le \sum_{k\in K} Q_k^{[i]}(\theta_k^{[i]T} - g\{p_k^{[i]}, h_k^{[i]}\}s_k^{[i]}\tau) \\
&\quad + V_K\sum_{k\in K} s_k^{[i]}p_k^{[i]}\tau,
\end{aligned} \tag{18}$$

$$\begin{aligned}
\widetilde{F_W}(\{p_w^{[i]}, s_w^{[i]}\}, \{p_l^{[i]}, s_l^{[i]}\}) &= \Delta(Q_w^{[i]}) + V_W\sum_{w\in W} s_w^{[i]}p_w^{[i]}\tau \\
&\le Q_w^{[i]L}\left[\sum_{l\in L} g(p_l^{[i]}, h_l^{[i]})s_l^{[i]}\tau \right. \\
&\quad \left. - g(p_w^{[i]}, h_w^{[i]})s_w^{[i]}\tau\right] \\
&\quad + V_W\sum_{w\in W} s_w^{[i]}p_w^{[i]}\tau + V_L\sum_{l\in L} s_l^{[i]}p_l^{[i]}\tau.
\end{aligned} \tag{19}$$

Eq. (19) can be reframed as

$$\begin{aligned}
\widetilde{F_W}(\{p_w^{[i]}, p_l^{[i]}, s_l^{[i]}\}) &\le \left\{Q_w^{[i]}\left[\sum_{l\in L} g(p_l^{[i]}, h_l^{[i]})s_l^{[i]}\tau \right.\right. \\
&\quad \left.\left. - g(p_w^{[i]}, h_w^{[i]})s_w^{[i]}\tau\right] + V_W P_w^{[i]}\right\} \\
\text{s.t.} V_L\sum_{l\in L} s_l^{[i]}p_l^{[i]}\tau &\le \text{Threshold.}
\end{aligned} \tag{20}$$

The optimization of the objective functions of Eqs. (19) and (20) can be rewritten as

$$\begin{aligned}
\min_{p_k^{[i]}} f_k &= V_K p_k^{[i]} - Q_k^{[i]} g\{p_k^{[i]}, h_k^{[i]}\}, \text{ s.t. } (2.11j) \\
&: \text{“}\forall\text{”} \quad k \in \mathscr{K},
\end{aligned} \tag{21}$$

$$\frac{\partial f_k}{\partial p_k^{[i]}} = V_k - \frac{\partial g\{p_k^{[i]}, h_k^{[i]}\}}{\partial p_k^{[i]}} Q_k^{[i]}. \tag{22}$$

From Eq. (21), we see the optimal setting of the directly connected IoTs.

$$\frac{\partial^2 f_w}{\partial P_w^{[i]} \partial p_l^{[i]}} = -Q_w^{[i]2} \frac{\partial^2 \sum g\{p_l^{[i]}, h_l^{[i]}\}}{\partial P_w^{[i]} \partial p_l^{[i]}} - Q_w^{[i]2} \frac{\partial^2 g\{p_w^{[i]}, h_w^{[i]}\}}{\partial P_w^{[i]} \partial p_l^{[i]}} + V_W \tag{23}$$

s.t. $V_L \sum_{l \in L} s_l^{[i]} p_l^{[i]} \tau \le$ Threshold.

While the last part of Eq. (23) can separated as

$$\min_{P_W} f_{w1} = V_W - \frac{\partial g(p_w^{[i]}, h_w^{[i]})}{\partial p_w^{[i]}} Q_w^{[i]}. \tag{24}$$

The first part of Eq. (23) we use the gradient scaled 0–1 Knapsack to optimize the power levels for the indirect IoTs. Thus, the problem becomes equivalent to solving the following gradient scaled 0–1 Knapsack:

$$\max \left[ \sum_{l=1}^{L} \left( \frac{\partial g\{p_l^{[i]}, h_l^{[i]}\}}{\partial p_l^{[i]}} \right) Q_l^{[i]} s_l^i \right] \text{ s.t. } V_L \sum_{l \in L} p_l^{[i]} \tau \le \text{Threshold}. \tag{25}$$

Since the above-mentioned segments of Eq. (23) are uncorrelated, the addition of their individual optimized value results in the optimal value for Eq. (23). Algorithm 1 provides the process flow for the proposed algorithm is given in Table 1.

**Table 1:** Algorithm 1

**Algorithm 1 – Power and scheduling process for the system**

***For each timeframe do***

**Phase 1: Power (at the individual device)**

for all $k \in K$ do

Calculate $(p_k^{[i]})^{\text{opt}}$ for maximal $f_k$ based on Eq. (22)

end

for all $l \in L$ do

Calculate $(p_l^{[i]})^{\text{opt}}$ for maximal of the knapsack problem based on Eq. (25)

end

**Phase 1: Scheduling (at the booster)**

Sort in the booster in ascending order

Set $(S_l^{[i]})^{\text{opt}}$ = 1 for the first N-A entries in the booster

Set $(S_l^{[i]})^{\text{opt}}$ = 0 for the remaining of the $L$ entries

Use the top $M$ of the data received for relay transmission in Phase 2, rest (N-A-M) data are stored in the booster queue

**Phase 2: Scheduling (at the gateway)**

Sort for transmission to the gateway

For the directly connected IoTs

Set $(S_k^{[i]})^{\text{opt}}$ = 1 for the first $N$ selected entries

For the Booster buoy

Set $(s_w^{[i]})^{\text{opt}} (S_w^{[i]})^{\text{opt}}$ = 1 for the first $M$ selected entries of the relay data of the booster buoy

End

## 2.3 Incorporation of RF energy

It is suggested to update the system design to include RF power transmission. We also include a dual period approach, whereby the first-time data transmission is accommodated from close sensors (within the grey circle's range in Figure 3), and the second-time data transfer is accommodated from distant sensors. Harvesting RF energy takes place throughout both time windows. Following that, the dual period periodicity is repeated. Algorithm 2 is provided for the process of the RF harvesting system, as indicated in Table 2.

# 3 Experimental results

A baseline demonstration will be built in this part to show how much energy our architecture uses. In order to determine the most efficient use levels, we will review the simulation findings for energy consumption, average packet latency, and average buffer space. Memory typically costs $0.02 per GB. We intend to place IoT devices with lots of memory in busy regions. Less memory will be available per device in less crowded places. Keeping energy usage to a minimum would further reduce the price of our architecture; 100 W will be the maximum gateway power transfer rate. There will only be ten power levels available for the gateway and IoT devices to use. The device ratio is another important metric used. The booster buoy ratio in relation to all IoT devices will be shown by the device ratio. The value has been set at 0.02, or 20%. For our simulations, a timescale parameter of 5,000 will be used. In the simulation, a random scheduling model [10] will be used; in this model, devices only transmit packets when their transmitting device's buffer level is not empty. Additionally, at the receiver where the signal was detected, the signal received must meet a certain signal intensity threshold value. Table 1 displays the simulation's inputs. Table 1 illustrates the presentation. For every power setting, the energy usage is shown in joules. The first five power settings have little energy use, as seen in the graph. At power level 7, there is a significant increase. The energy consumption increases after the rise and peaks at slightly under 2 J. Our initial assessment indicates that when the rate ratio and average buffer space rise, so does the quantity of energy used. We provide a table of the simulations we carry out,

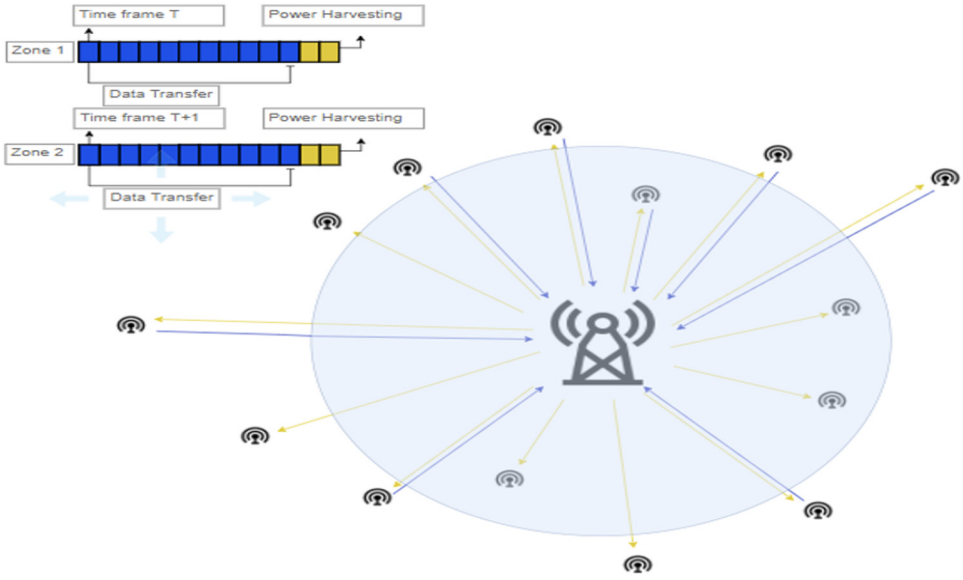


**Figure 3:** Dual period system diagram.

**Table 2:** Algorithm

| **Algorithm 2** |
|---|
| for each timeframe **do** |
| **Phase 1: Power Allocation** |
| **for all** $k \in \mathcal{K}$ zone 1 **do** |
| if timeframe even use zone 1 devices |
| if timeframe odd use zone 2 devices |
| (if multiple zones used) |
| Calculate$(p_k^{[i]})^{(\text{"opt)"}}$ |
| Evaluate $f_1$ |
| Store obtained value of $f_1$ in matrix $X$ |
| **end for** |
| **Phase 2: Scheduling** |
| Sort $X$ in ascending order |
| Set $s_k^{[i]}$= 1 for first $N$ entries in $X$ |
| Set $s_k^{[i]}$= 0 for the rest of the entries in $X$ |
| **Phase 3: Device Queue Update** |
| Update $Q_k^{[i]} \forall k \in \mathcal{K}$ zone1 |
| Update $Q_k^{[i]} \forall k \in \mathcal{K}$ zone2 |
| Update $E_k^{([i],\text{tot})} \forall k \in \mathcal{K}$ zone 1 |
| Update $E_k^{([i],\text{tot})} \forall k \in \mathcal{K}$ zone 2 |

to represent different series of experimentations, as shown in Table 3.

The characteristics in Table 4 are used in the baseline demonstration below. For each power level, the energy consumption is shown in joules in Figure 4. The first five power settings have little energy use, as seen in the graph. At power level 7, there is a significant increase. The energy

**Table 3:** Simulation parameters

| **Parameters** | **Value** |
|---|---|
| Max distance from IoT to gateway | 2 km |
| Max distance from IoT to buoy | 3 km |
| Distance from galaxy to satellite | 800 km |
| Tier1 path loss | 4 |
| Tier2 path loss | 2.5 |
| Noise variance | −174 dBm/Hz |
| Detection Threshold at gateway | −7 dB |
| Timeframe length | 10 ms |
| Power | 790 mW |
| Number of IoT device | 250 |
| Device ratio | 0.2 |
| Length of a packet | 168 bits |

consumption increases after the rise and peaks at slightly under 2 J. Our initial assessment indicates that when the rate ratio and average buffer space increase, so does the quantity of energy used.

## 3.1 Simulation I

Two factors were changed in this simulation to examine how our data would change. The quantity of traffic on the network grew along with the growth in IoT devices from 250 to 500. These adjustments were made to take into account the fact that a significant portion of the marine creatures being monitored by our equipment are tagged.

**Table 4:** Experimentation scenarios

| Simulation | Monitoring region | Traffic level | Motivation | Energy consumption |
|---|---|---|---|---|
| I | Large | High | Marine life near shipping channels | High |
| II | Large | Low | Marine life around coral reef | Medium |
| III | Small | High | Sea turtles nesting eggs | Medium to High |
| IV | Small | Low | Marine life in Cold Water | Low |

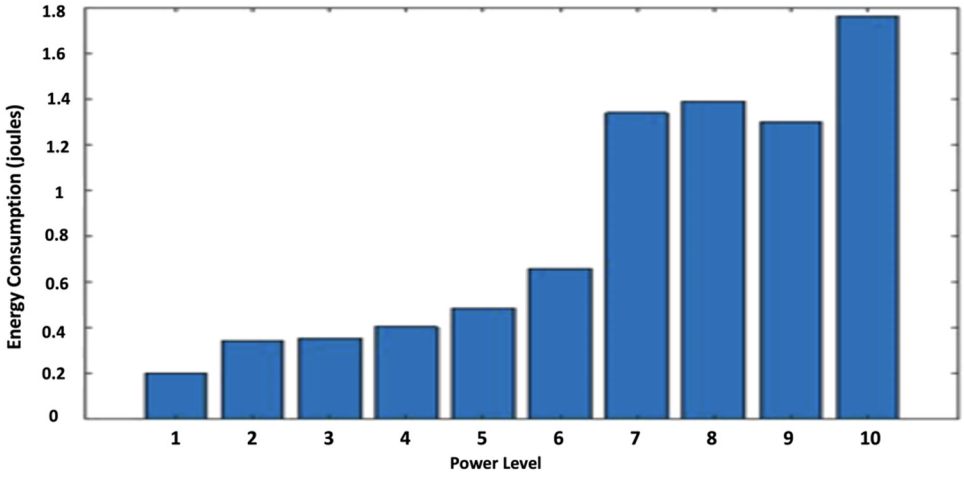


**Figure 4:** The energy consumption for different power levels.

The data that differ from our baseline example is shown in detail in Figure 5. The energy usage is significantly greater than our baseline figure due to the rise in IoT devices. Energy usage increases when the average buffer level rises.

## 3.2 Simulation II

We changed the same two parameters from simulation I to simulation II; 500 IoT devices are present. However, there is less load on the network now. The disparity between the data readings from our baseline demonstration and our first simulation is shown in detail in Figure 6. The average buffer levels are stable and much lower than in simulation I as a result of the drop in network traffic.

## 3.3 Simulation III

We changed the same two parameters from our first simulation to our third simulation. The network's traffic grew while the number of IoT devices was reduced from 500 to 50. The disparity between the data readings from our baseline demonstration and earlier models is shown in detail in Figure 7. This simulation uses a little bit more energy than our reference reading. This simulation shows that the volume of traffic also has a significant impact on energy consumption levels. With an average packet delay of about one millisecond, there is hardly any latency.

## 3.4 Simulation IV

The identical settings that were changed before were used for our most recent simulation. The quantity of traffic on the network was reduced, and the number of IoT devices was reduced from 500 to 50. The disparity between the data readings from our baseline demonstration and earlier models is shown in detail in Figure 8. All three of our graphs are altered when one of the two parameters is decreased. The average buffer space level is about the same as it was in our second experiment during the period of lower network traffic. The amount of buffer space is still about eight packets.

The cases that were simulated were actual ones where IoT monitoring would be useful. It is also important to evaluate the IoT devices' memory and storage

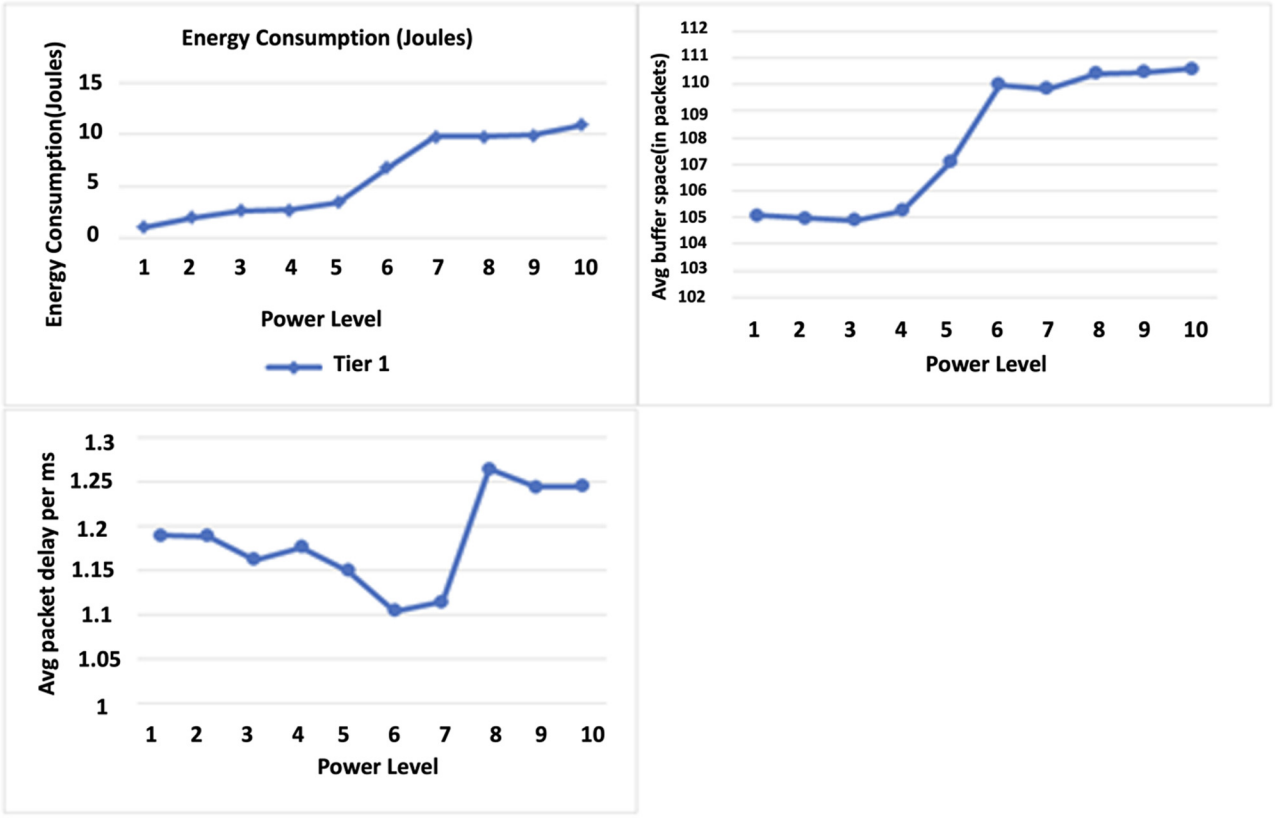


**Figure 5:** Simulation I data change.

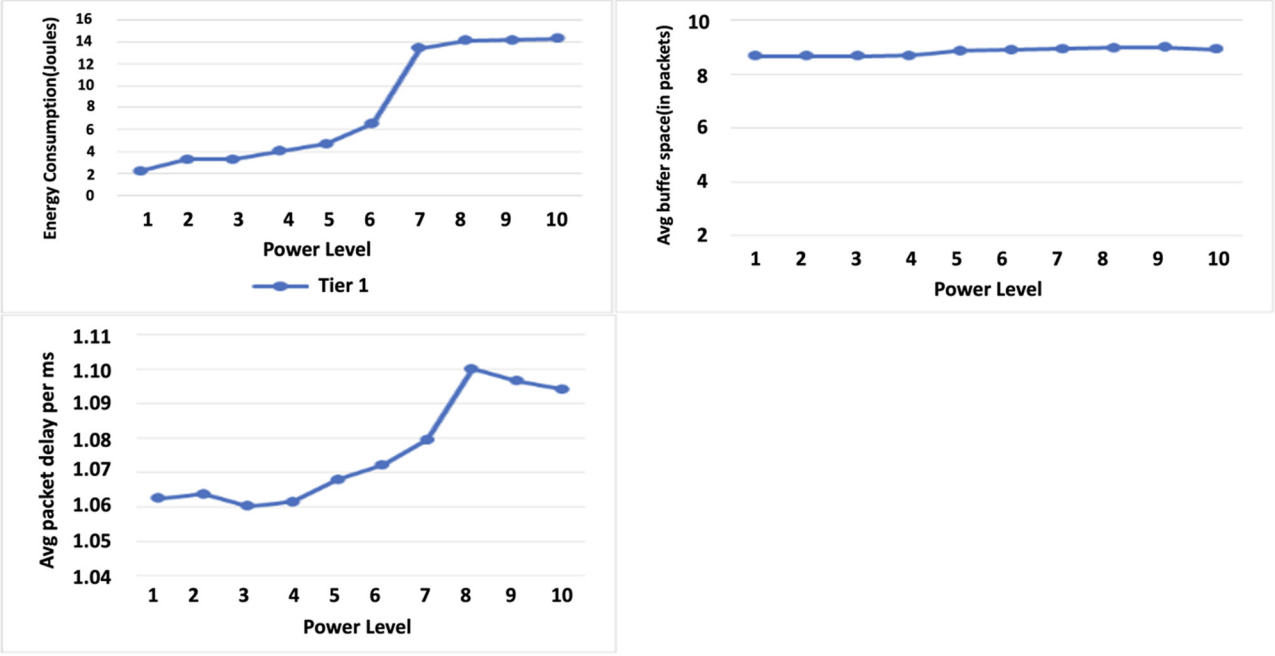


**Figure 6:** Simulation II data change.

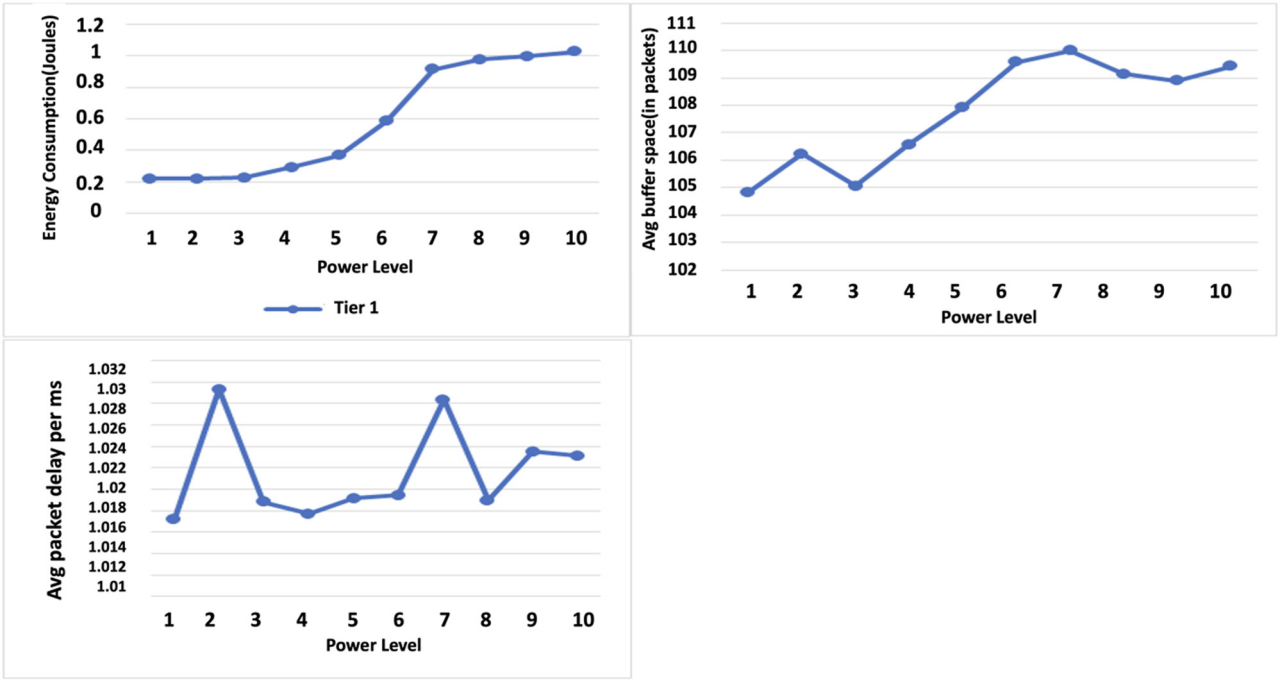


**Figure 7:** Simulation III data change.

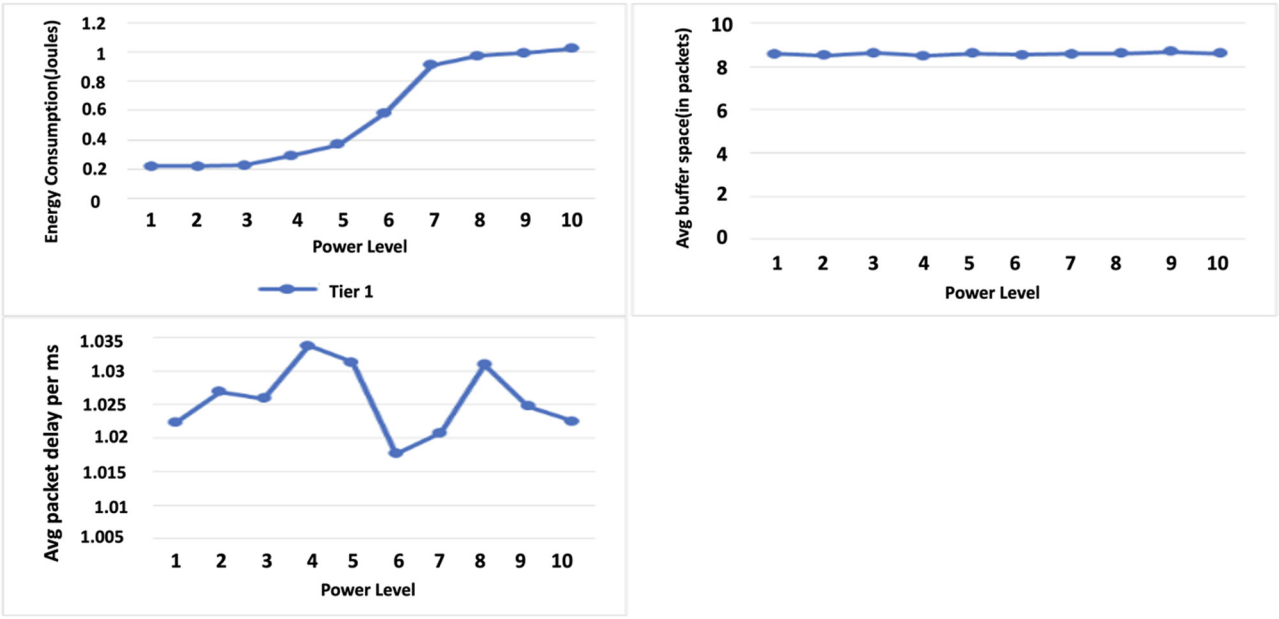


**Figure 8:** Simulation IV data change.

requirements as well as their price and quantity. For each of the simulations that were run, suggestions and future projections are shown in Table 5. Additionally, we provide the outcomes of the two instances of RF energy harvesting integration for IoT devices. We describe the two situations in more detail and offer the outcomes.

**Table 5:** Simulation expectations

| Simulation | Monitoring region | Traffic level | Motivation | Energy consumption | Recommended IoT device |
|---|---|---|---|---|---|
| I | Large | High | Marine life near Shipping channels | High | Expensive, fault-tolerant, low quantity of device |
| II | Large | Low | Marine life around coral reef | Medium | Inexpensive, memory/storage intensive, high quantity of device |
| III | Small | High | Sea turtles nesting eggs | Medium to high | Expensive, fault-tolerant, high quantity of device |
| IV | Small | Low | Marine life in Cold Water | Low | Inexpensive, large amount of memory, high quantity of device |

## 3.5 RF energy harvesting IoT Case I

For each interval, we use 400 devices with 100 transmitting slots. In Case I, all devices are qualified to transmit; 500 periods with $\_m$ equal to 5, 10, 15, 20, 25, and 30% are run through this. Using even costs for data and energy as well as greater and lower costs for data to energy, the program is conducted as given in Figure 9. Average buffer length, under conditions of equal costs for data transmission and energy consumption in an IoT network, refers to the typical amount of data waiting to be sent from devices to a central hub or the cloud. It represents a balance between data accumulation and energy expenditure, ensuring the network's efficiency and sustainability. In this scenario, the network aims to maintain an equilibrium, minimizing the time data spends in device buffers while avoiding excessive energy usage. Achieving an optimal average buffer length is essential for preserving device battery life and maintaining data flow, ultimately maximizing the network's performance and resource utilization.

In Figure 10, we employ 400 devices with 100 transmitting slots for every interval. Every device is eligible to transmit in Case I. This is done for 500 periods with $\_m$ equal to 5, 10, 15, 20, 25, and 30%. The average number of scheduled requests, with uniform costs for data and energy, refers to the expected frequency at which IoT devices in a network request scheduling for data transmission to a central hub. In this context, data and energy are equally valued, and devices seek an optimal balance. Maintaining a manageable average number of requests is crucial for minimizing network congestion and conserving device energy. It ensures that devices efficiently and fairly access the network while avoiding unnecessary overhead. Striking this balance is essential for achieving efficient data transmission, preserving energy resources, and promoting equitable communication within the IoT ecosystem.

In Figure 11, we analyze the energy consumption for $\_m$ equal to 5, 10, 15, 20, 25, and 30%. In an IoT system, total energy consumption is the total amount of energy used by all devices for network operations and data transmission, assuming that data and energy costs are equal. The objective in this case is to strike a balance between the energy costs and the advantages of data transfer. The network can guarantee sustainability and longer device battery life while ensuring effective data transfer by optimizing total energy consumption. Reaching this balance reduces needless energy waste, making the IoT infrastructure more economical and ecologically benign. Achieving optimal equilibrium in overall energy usage is crucial for the network's sustainability and effectiveness in the long run.

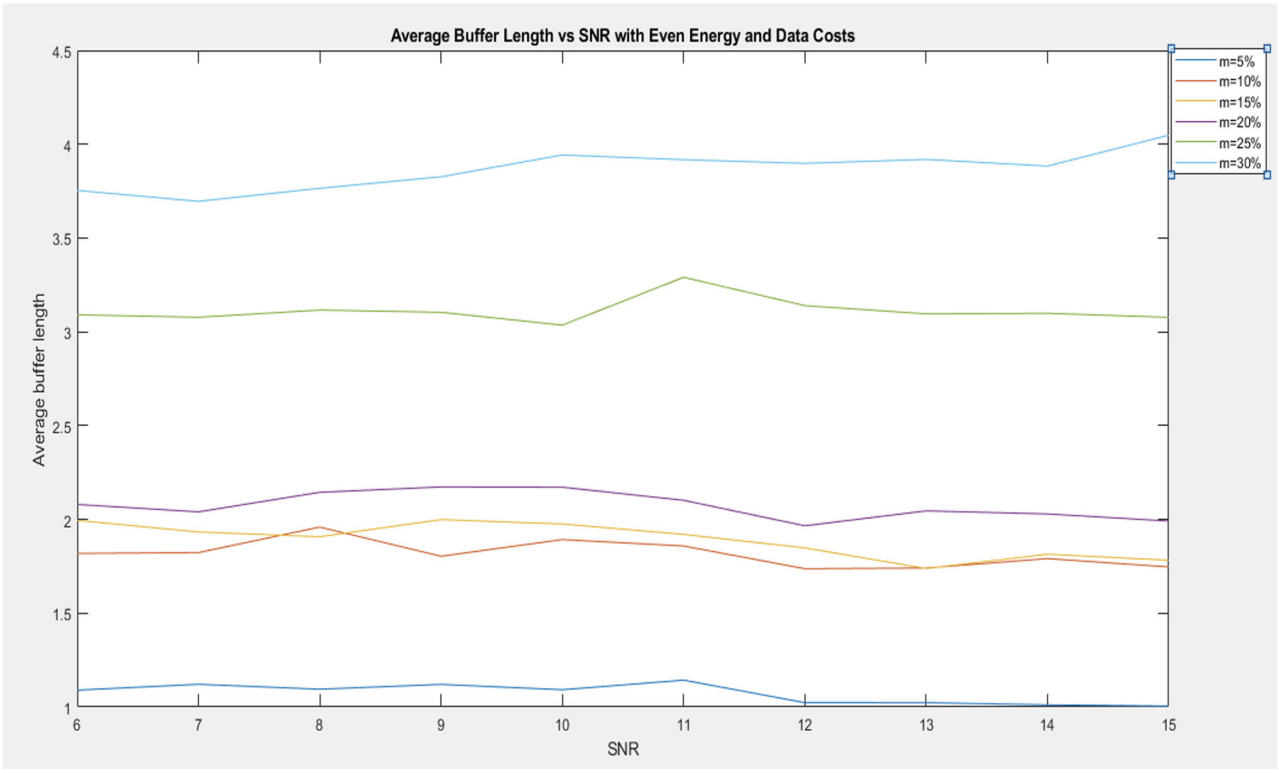


**Figure 9:** Average buffer length with even costs for data and energy.

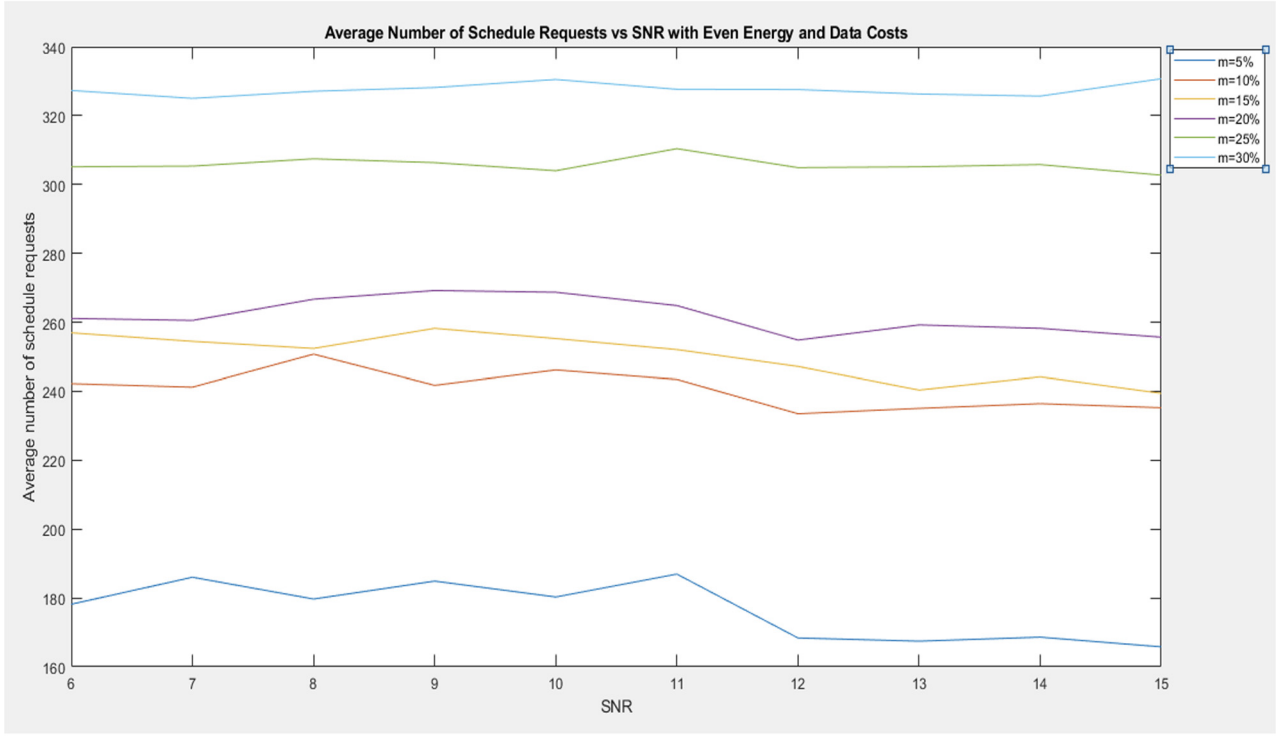


**Figure 10:** Average number of schedule requests with even costs for data and energy.

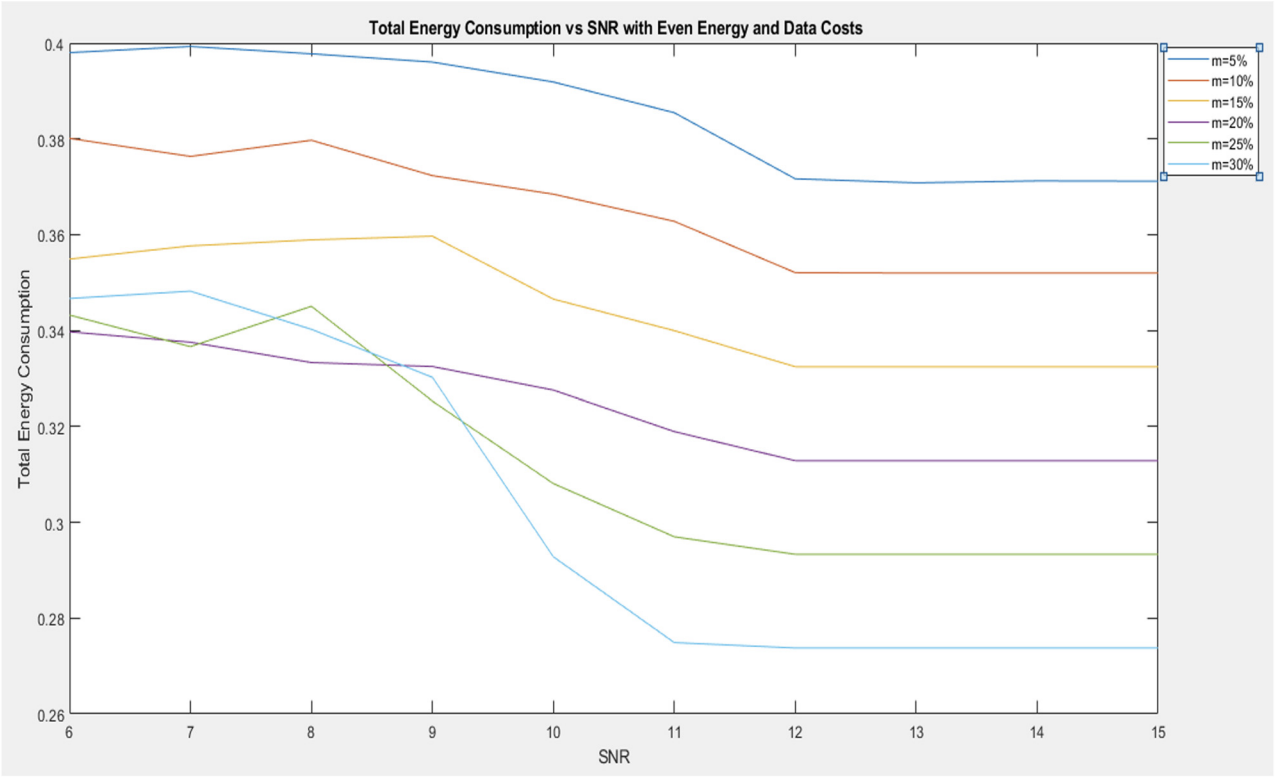


**Figure 11:** Total energy consumption with even costs for data and energy.

In Figure 12, we estimate the energy consumption of scheduled devices *vs* signal-to-noise Ratio (SNR) for *_m* equal to 5, 10, 15, 20, 25, and 30%. The total energy consumption of scheduled devices *vs* SNR in the context of even energy and data costs in an IoT network represents an important trade-off. As SNR increases, devices require less energy to transmit data reliably, but scheduling decisions may become more complex. Scheduled devices aim to minimize energy consumption, as each transmission consumes power, while SNR reflects the quality of the communication channel. Balancing these factors optimally is essential. Devices with good SNR can transmit with lower energy consumption, but effective scheduling of all devices is necessary to maintain network performance and energy efficiency. Striking this balance ensures reliable data transmission with minimal energy usage, maximizing the overall network's efficiency and effectiveness.

In Figure 13, we estimate the performance of buffer length *vs* SNR for *_m* equal to 5, 10, 15, 20, 25, and 30%. The performance of buffer length *vs* SNR for different percentages of available memory (*_m*) in an IoT network reveals crucial insights. As *_m* increases from 5% to 30%, the network's buffer capacity expands. With higher SNR, data transmission becomes more reliable, and devices with larger buffer lengths can capitalize on better channel conditions. This relationship highlights the trade-off between buffer size and SNR. Smaller buffers may experience more data loss in low SNR scenarios, while larger buffers can absorb and transmit more data. Optimal performance lies in adapting buffer length based on SNR and the specific memory resources available, ensuring efficient data transmission while minimizing potential data loss.

The average number of schedule requests *vs* SNR in the context of lower energy costs for data transmission than for data processing and storage (*_m* ranging from 5 to 30%) reveals an intriguing dynamic as given in Figure 14. Lower energy costs for data favor more frequent schedule requests, as devices seek to transmit data more often. A higher SNR allows for more reliable data transmission, reducing the urgency of scheduling. As *_m* increases, devices with more available memory may request schedules more frequently. The key is finding a balance that optimizes scheduling efficiency while considering the energy trade-offs, SNR conditions, and the specific memory constraints of the IoT network.

A crucial trade-off in IoT networks is between total energy consumption and SNR as given in Figure 15, particularly when data transmission has lower energy costs (*_m* ranging from 5 to 30%) than data processing and storage. Devices are incentivized to communicate more frequently

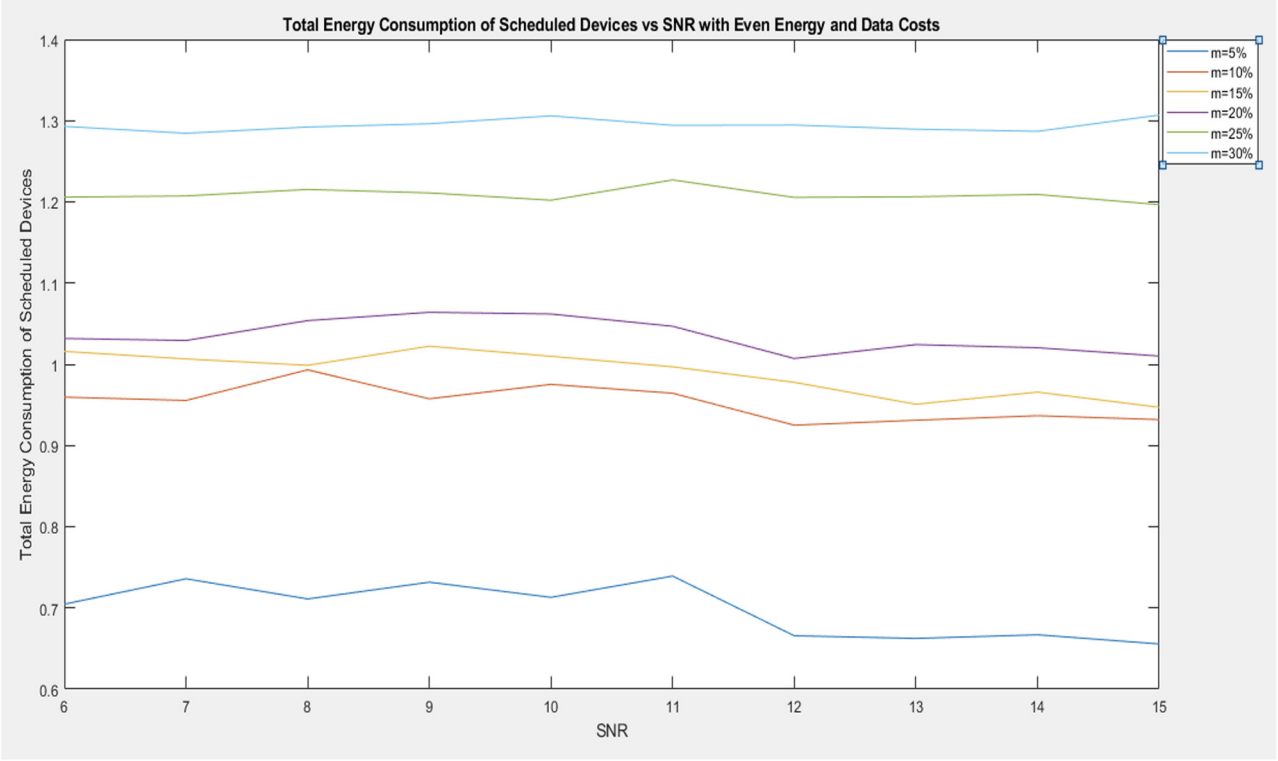


**Figure 12:** Total energy consumption of scheduled devices *vs* SNR with even energy and data cost.

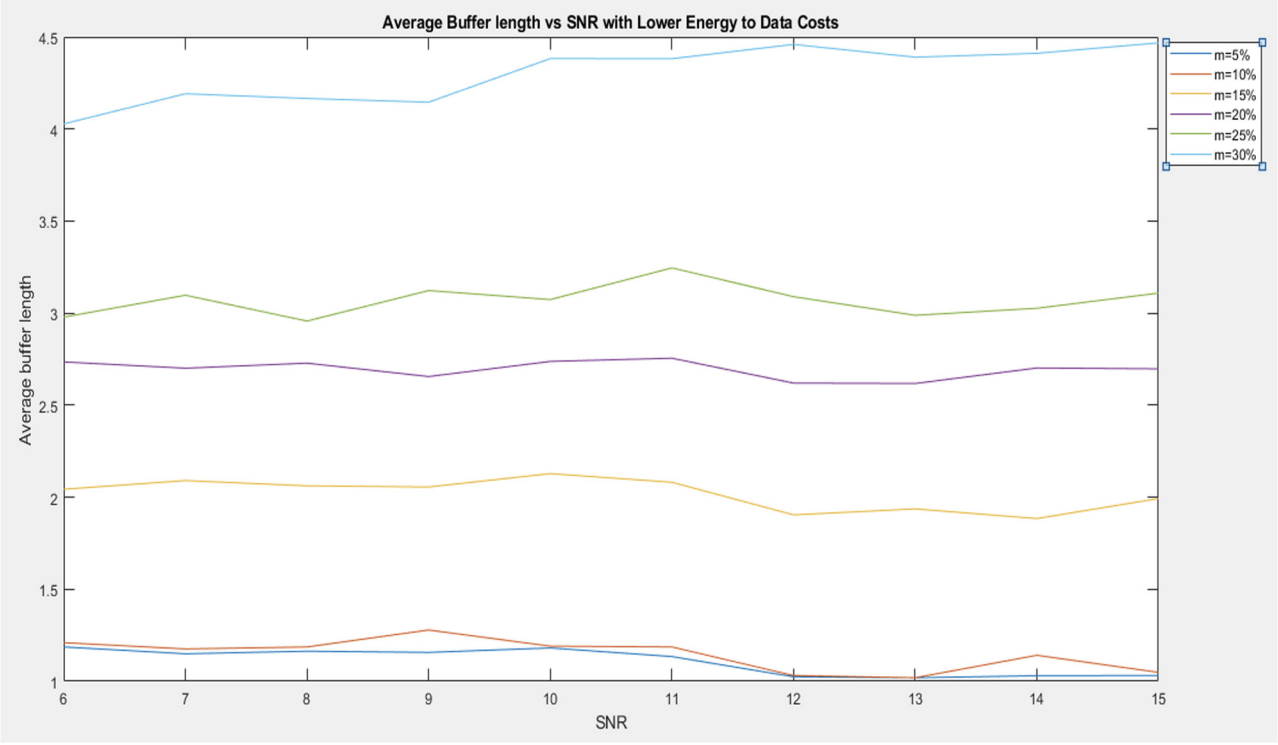


**Figure 13:** Average buffer length *vs* SNR with lower energy costs than data.

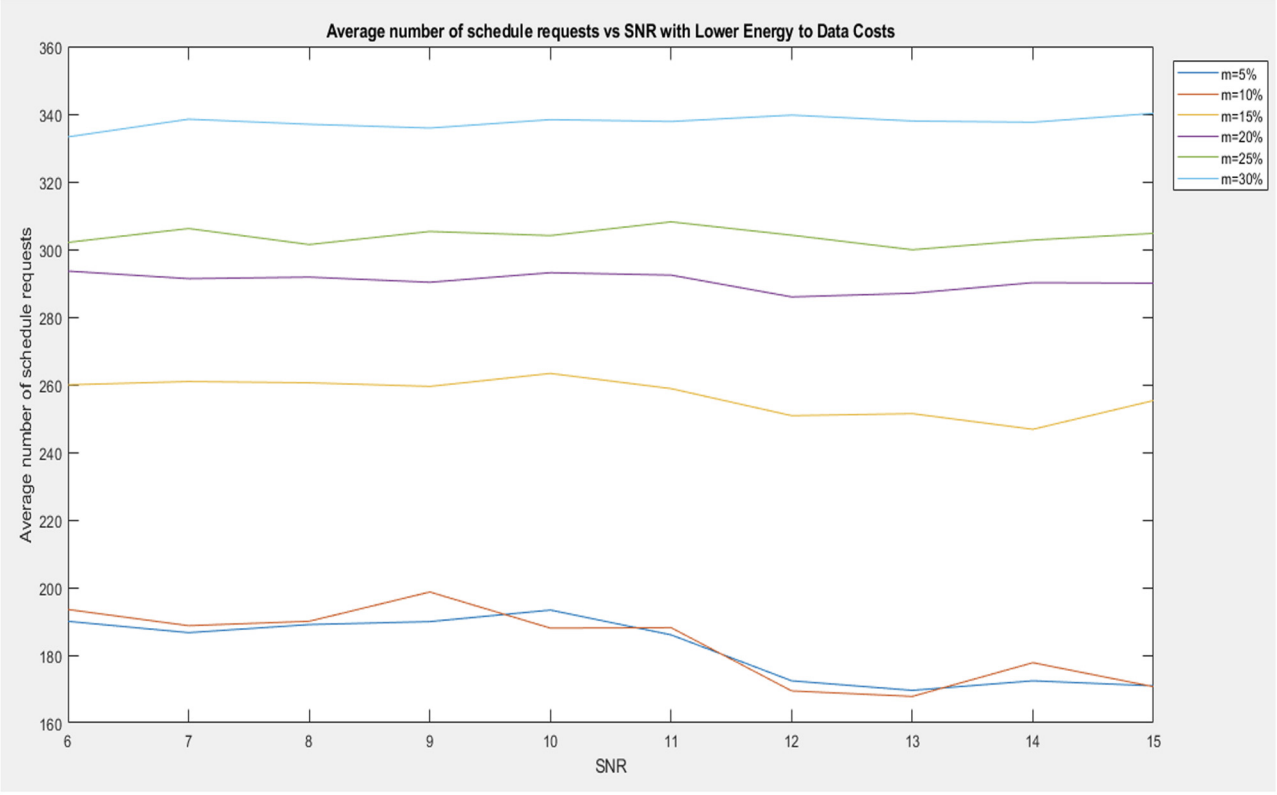


**Figure 14:** Average number of schedule requests *vs* SNR with lower energy costs than data.

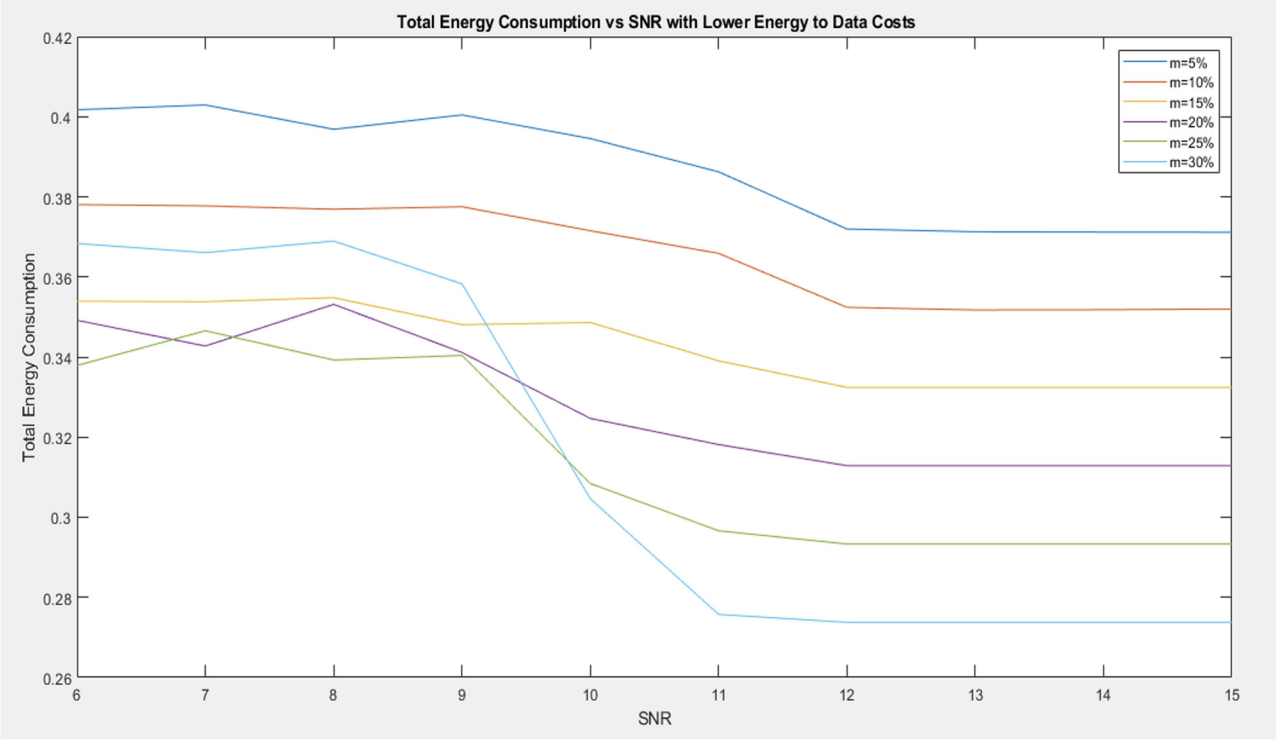


**Figure 15:** Total energy consumption with *vs* SNR lower energy costs than data.

when data transmission energy prices decrease. Data transmission becomes more energy-efficient with a greater SNR. Devices with higher memory capacities can afford to buffer data as _*m* grows, perhaps leading to fewer, more energy-efficient transfers. This equation must be balanced in order to decrease total energy consumption and provide reliable data communication in the IoT ecosystem. Lower data energy costs must be assessed against SNR conditions and memory limits.

Figure 16 indicates the total energy consumption of scheduled devices, in the context of lower energy costs for data transmission than for data processing and storage (_*m* varying from 5 to 30%), representing an intricate relationship. As _*m* increases, devices with more available memory can afford larger buffers, allowing them to schedule transmissions less frequently. With lower energy costs for data, devices may favor more frequent scheduling. Moreover, the SNR influences the energy efficiency of scheduled data transmissions. The optimal balance is achieved by considering _*m*, SNR conditions, and energy trade-offs. Reducing data transmission costs while efficiently utilizing device memory is vital to minimize energy consumption while ensuring reliable data transfer in IoT networks.

The average buffer length *versus* SNR in the context of higher energy costs for data processing and storage compared to data transmission (_*m* ranging from 5 to 30%) reflects an intriguing interplay as demonstrated in Figure 17. In situations with elevated energy costs for data handling, devices may prefer to keep smaller buffers to reduce data storage and processing. A higher SNR allows for more reliable data transmission, influencing the necessary buffer size. As _*m* increases, devices with more memory capacity can maintain larger buffers. Achieving the optimal average buffer length entails striking a balance between SNR, energy trade-offs, and memory constraints, ensuring efficient data processing while minimizing energy consumption in the IoT network.

Figure 18 represents a complex link when examining the average number of scheduling requests *vs* SNR in the setting of higher energy expenditures for data processing and storage than for data transmission (_*m* changing from 5 to 30%). Devices are encouraged to avoid scheduling requests due to the higher energy costs associated with data processing, particularly in low SNR conditions where data dependability is impaired. Devices with higher memory resources can afford to buffer data and make fewer scheduling requests as _*m* rises. It is crucial to strike the ideal balance between the quantity of scheduling requests and SNR levels. This allows for different memory limits in the IoT ecosystem while guaranteeing effective data management, reducing energy consumption, and maintaining network speed.

Figure 19 estimates the total energy consumption with respect to SNR. Considering SNR and higher energy costs

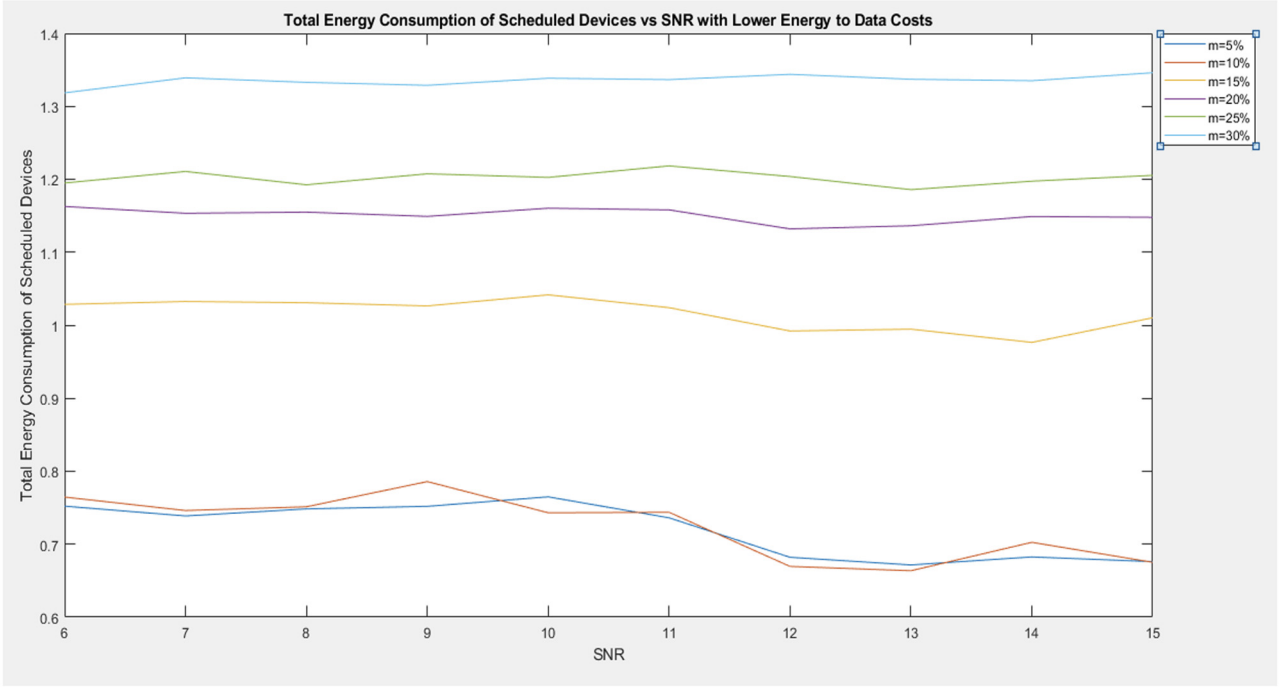


**Figure 16:** Total energy consumption of scheduled devices *versus* with lower energy costs than data.

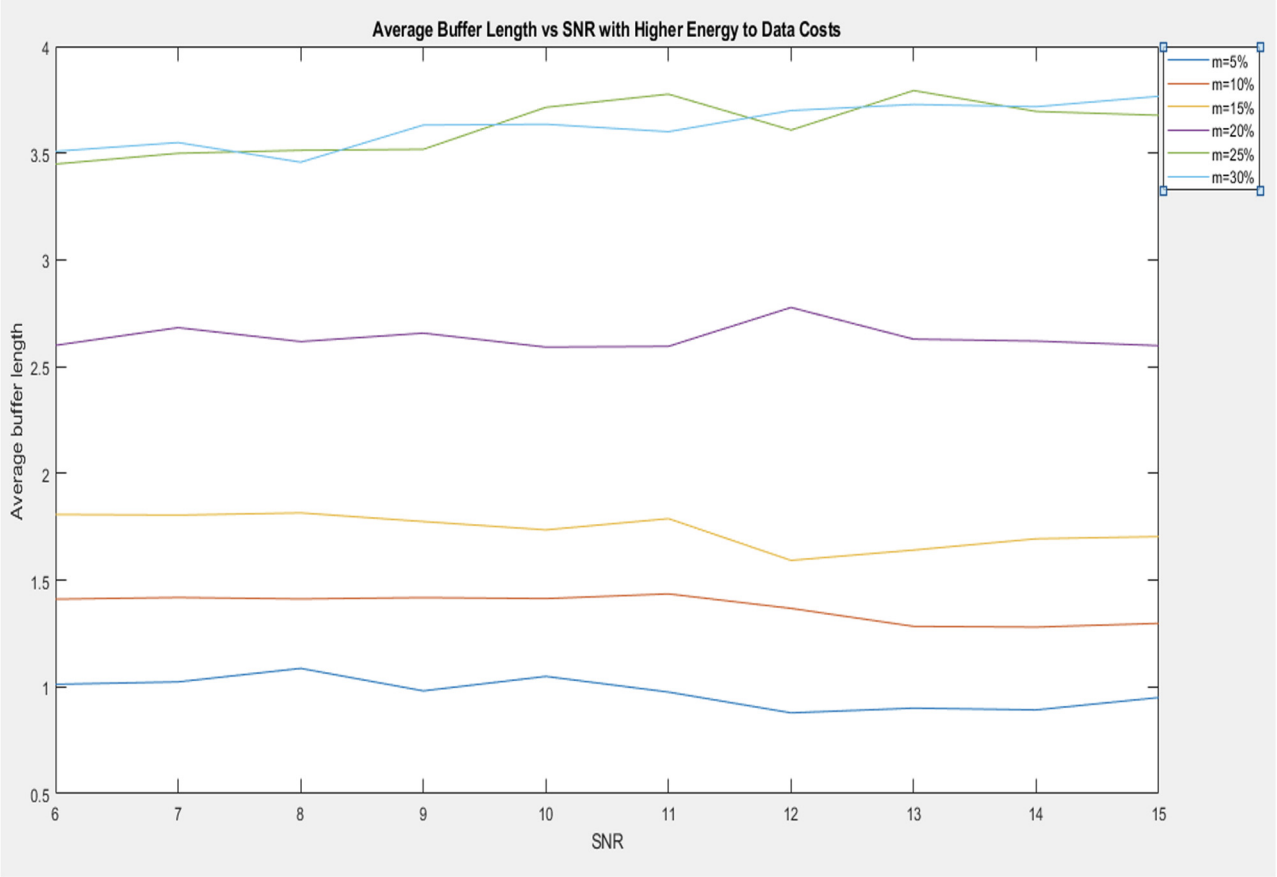


**Figure 17:** Average buffer length *vs* SNR with higher energy costs than data.

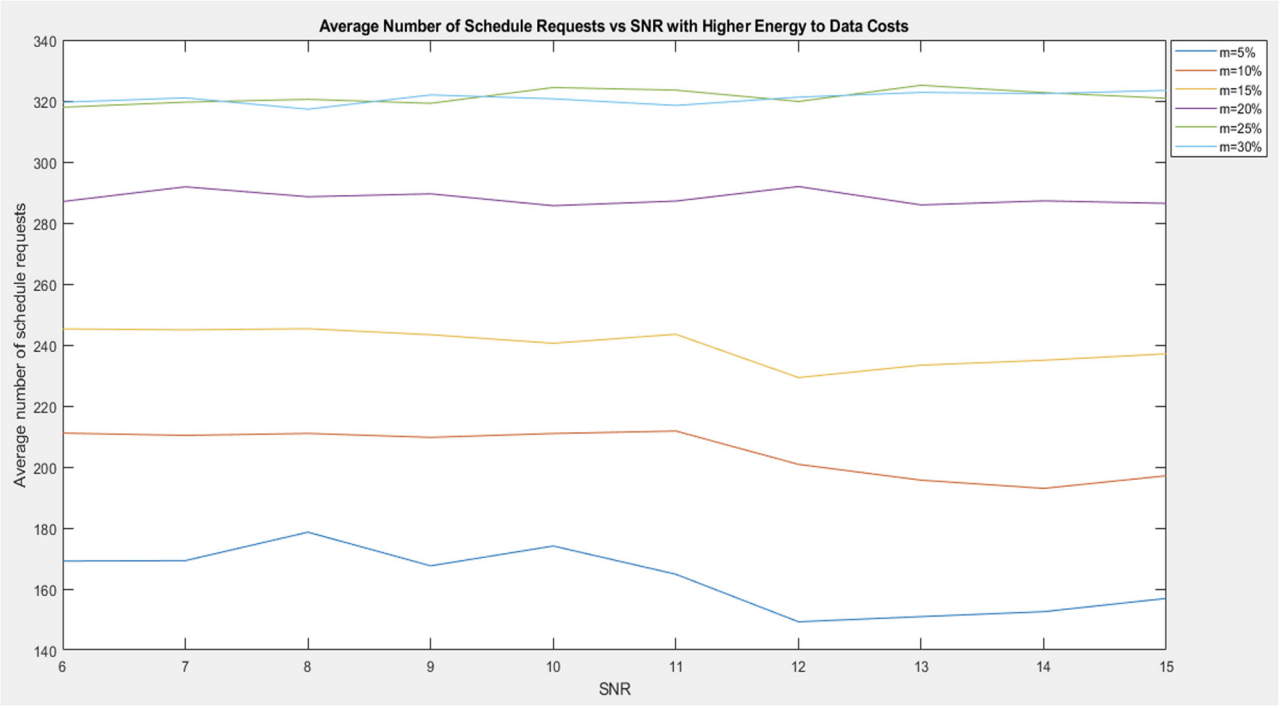


**Figure 18:** Average number of schedule requests *vs* SNR with higher energy costs than data.

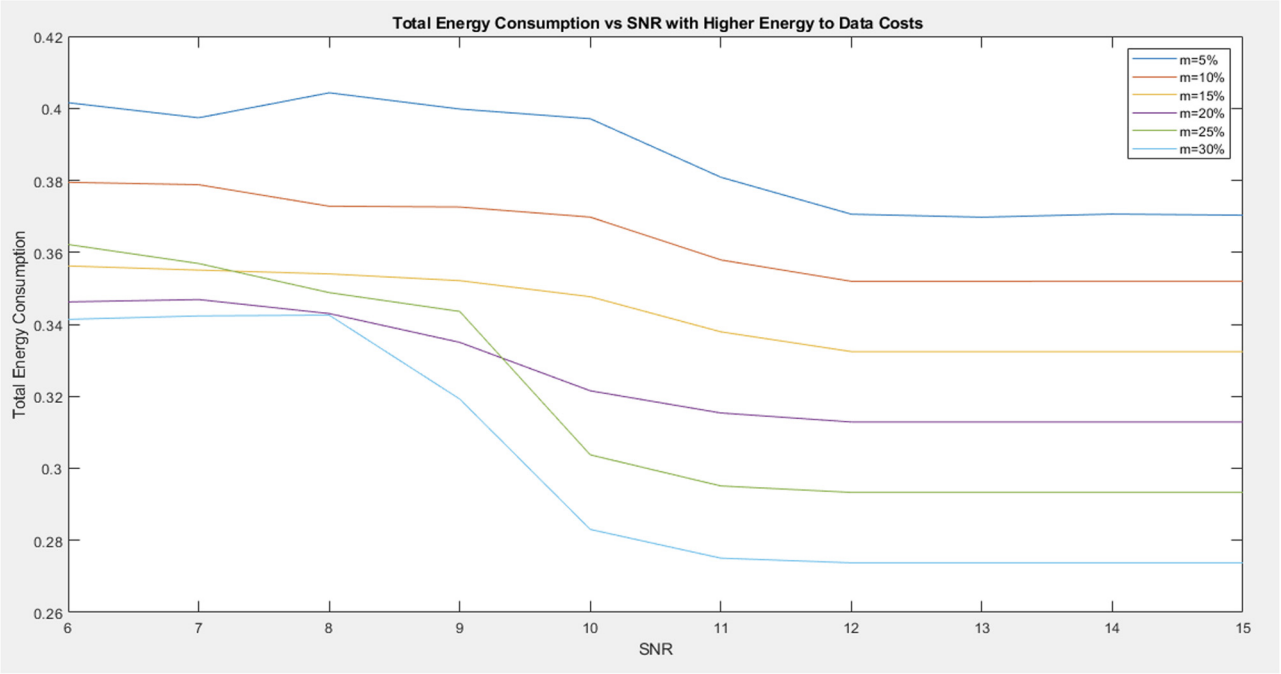


**Figure 19:** Total energy consumption with higher energy costs than data.

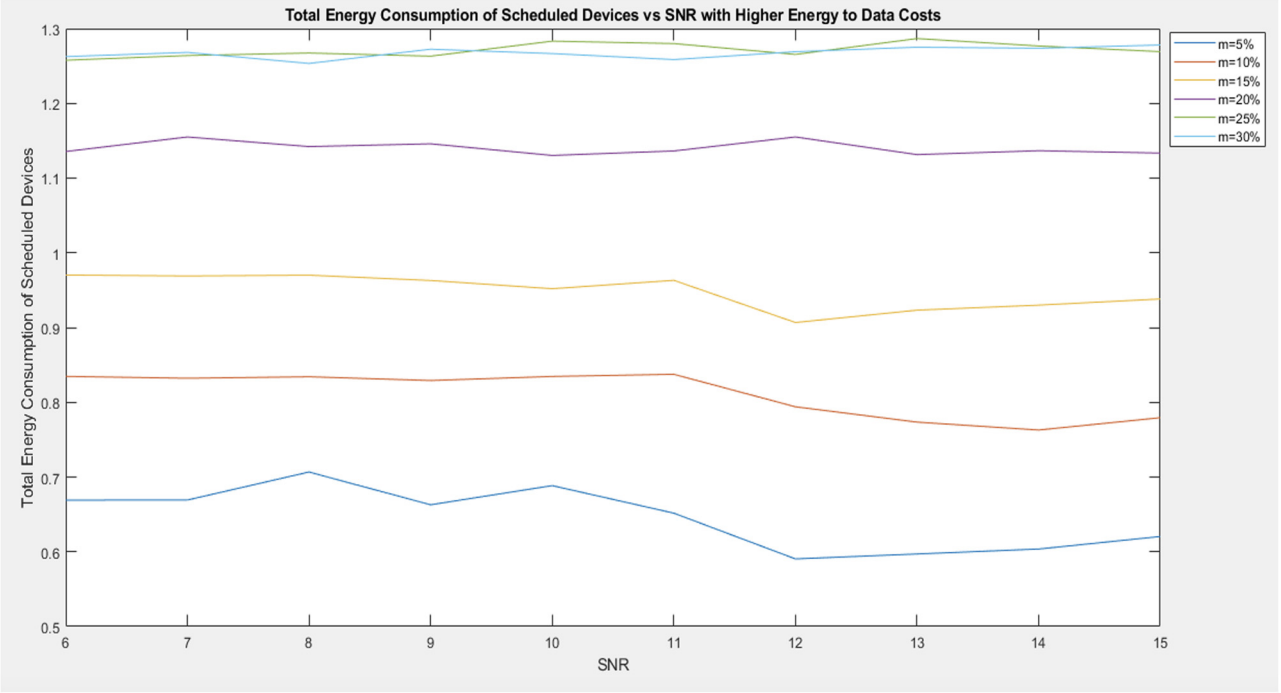


**Figure 20:** Total energy consumption of scheduled devices with higher energy costs than data.

for data processing than for data transmission, total energy consumption is a measurement of the overall energy used in an IoT network. The energy balance changes when _$m$ fluctuates between 5 and 30%. Higher data processing costs drive more efficient scheduling and data management strategies to save energy. A higher SNR maximizes energy economy and implies more reliable data transmission. In order to get the ideal balance, energy consumption must be

adjusted to SNR levels, memory constraints, and the number of devices that can transmit data at the same time. By doing this, the IoT network's energy resources are preserved, and reliable and efficient data transmission is ensured.

Figure 20 estimates the total energy consumption of scheduled devices with higher energy costs for data processing and storage compared to data transmission signifies the overall power expenditure required to manage and transmit data in an IoT network. In this scenario, devices aim to conserve energy, often by buffering data to reduce the frequency of data transmissions. This approach lowers the energy cost associated with transmission but increases the energy consumed for data management. Striking a balance between these two energy components is critical to optimize overall energy consumption. By efficiently managing data, scheduling transmissions, and minimizing energy-intensive processes, the network can maintain data reliability while conserving power, enhancing the sustainability and longevity of the IoT ecosystem.

## 3.6 RF energy harvesting IoT Case II

Next, we employ 400 devices once more, but only 100 of them can send data at a time. In this scenario, only nearby devices can broadcast during odd periods, whereas distant devices can only send during even periods. Throughout, RF harvesting may be placed; 500 periods with $\_m$ equal to 5, 10, 15, 20, 25, and 30% are run through this. Using even costs for data and energy as well as greater and lower costs for data to energy, the program is conducted. The data may be found in the following Figures 21–28.

In Figure 22, we use 400 devices again, but only 100 of them have data-sending capability. In this case, faraway devices can only send during even time intervals, whereas nearby devices can only broadcast during odd time periods. RF harvesting may occur throughout. This is done for 500 periods where $\_m$ is 5, 10, 15, 20, 25, and 30%. The program is run using even costs for energy and data, as well as higher and lower costs for data and energy. The frequency at which IoT devices look for scheduling for data transmission is reflected in the average number of scheduled requests, with equal expenses for data and energy. Devices try to balance energy savings and effective data transmission in this case of equal data and energy expenses, maximizing network performance.

For 400 devices again, but only 100 of them have data-sending capability, the performance of total energy consumption *vs* SNR is given in Figure 23. In the context of uniform costs for data and energy, when only a limited number of devices can transmit data simultaneously ($\_m$ ranging from 5 to 30%), this reflects the cumulative energy

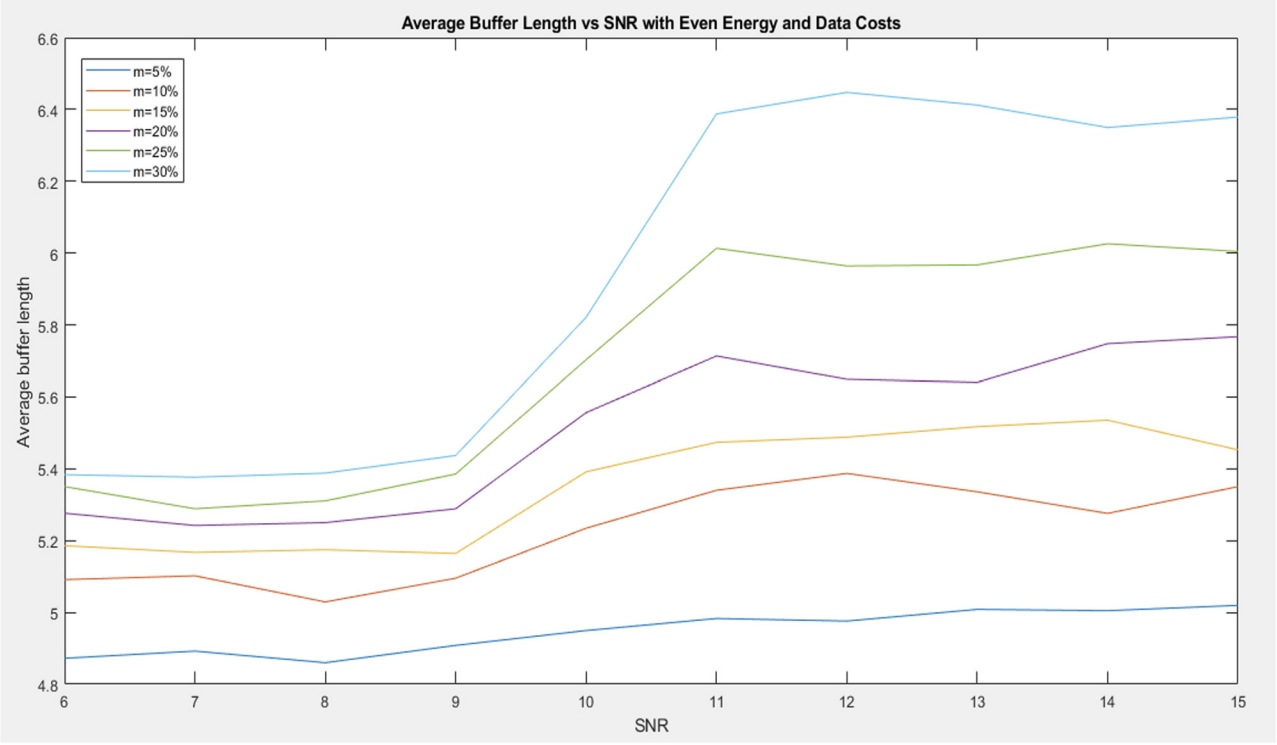


**Figure 21:** Average buffer length with even costs for data and energy.

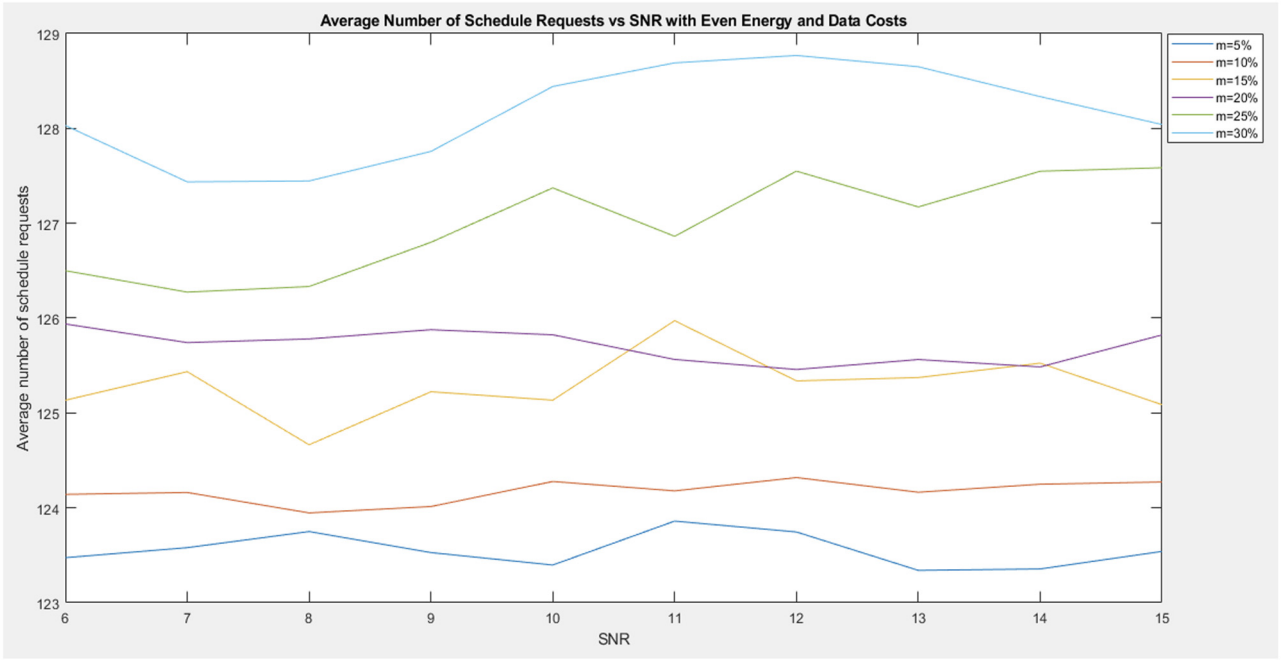


**Figure 22:** Average number of schedule requests with even costs for data and energy.

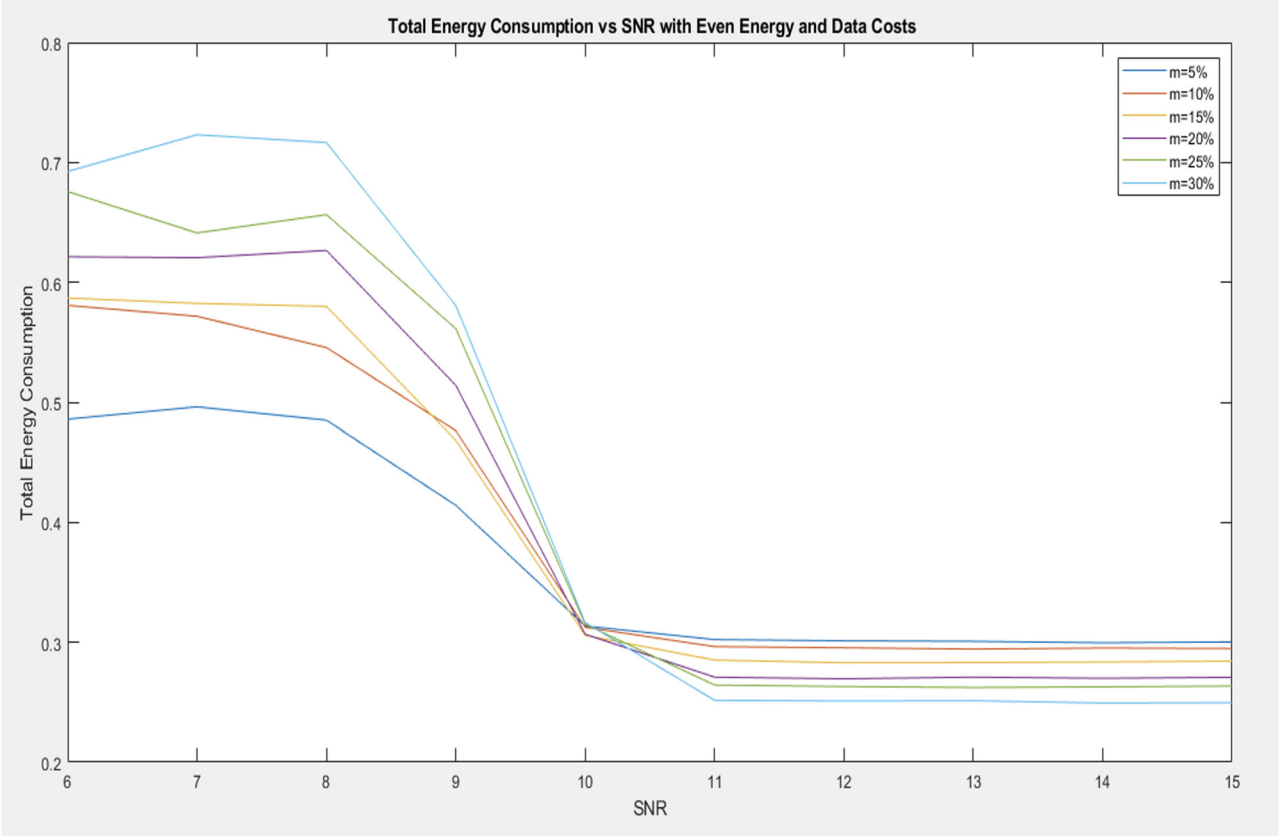


**Figure 23:** Total energy consumption with even costs for data and energy.

utilized for data transfer. As _*m* increases, more devices can transmit concurrently, potentially reducing the time data spends in buffers. This can lead to more efficient energy utilization but also a higher potential for network congestion. Striking the right balance is crucial; it involves optimizing data transmission while considering energy trade-offs, the number of devices transmitting simultaneously, and network performance to ensure efficient and reliable operation in IoT systems.

Given a limited number of concurrent device transmissions (_*m* between 5 and 30%) and lower energy costs for data processing and storage, the total energy consumption of scheduled devices relative to SNR that represents the energy used for data management and transmission is represented in Figure 24. It is imperative to maximize scheduling because there are not as many devices broadcasting at once. Devices are encouraged to transmit more frequently by lower data transmission costs, while effective data transfer is encouraged by better SNR. Finding the ideal balance in IoT networks with limited simultaneous transmission capacity requires adjusting scheduling, taking SNR conditions into account, and making energy trade-offs in order to provide dependable data transmission while preserving energy resources.

Figure 25 indicates the average buffer length indicates the normal amount of data that is waiting to be transmitted IoT devices, given the greater energy costs associated with data management as opposed to data transmission and the limited number of concurrent device transmissions (_*m* ranging from 5 to 30%). Maintaining a balanced buffer length is essential when there are fewer devices transmitting simultaneously. Smaller buffer sizes may be encouraged by higher data management expenses to lower processing requirements. In order to provide effective data processing and dependable communication within the IoT network, achieving an ideal buffer length requires careful consideration of energy trade-offs, memory limitations, and the number of devices capable of simultaneous data transmission.

The average schedule request count in relation to SNR in a case, where data processing energy costs are higher than data transmission energy costs and only a small number of concurrent device transmissions (_*m* ranging from 5 to 30%) are supported, emphasizes how difficult it is to schedule in IoTs networks is shown in Figure 26. When fewer devices are transmitting simultaneously, effective scheduling is required. Devices might make more thoughtful scheduling requests if data processing costs are higher. Data transmission that uses less energy is encouraged by a greater SNR. In order to ensure reliable communication while preserving energy resources in constrained concurrent transmission situations, scheduling must be adjusted to SNR conditions, energy trade-offs, and the number of devices capable of simultaneous data transmission.

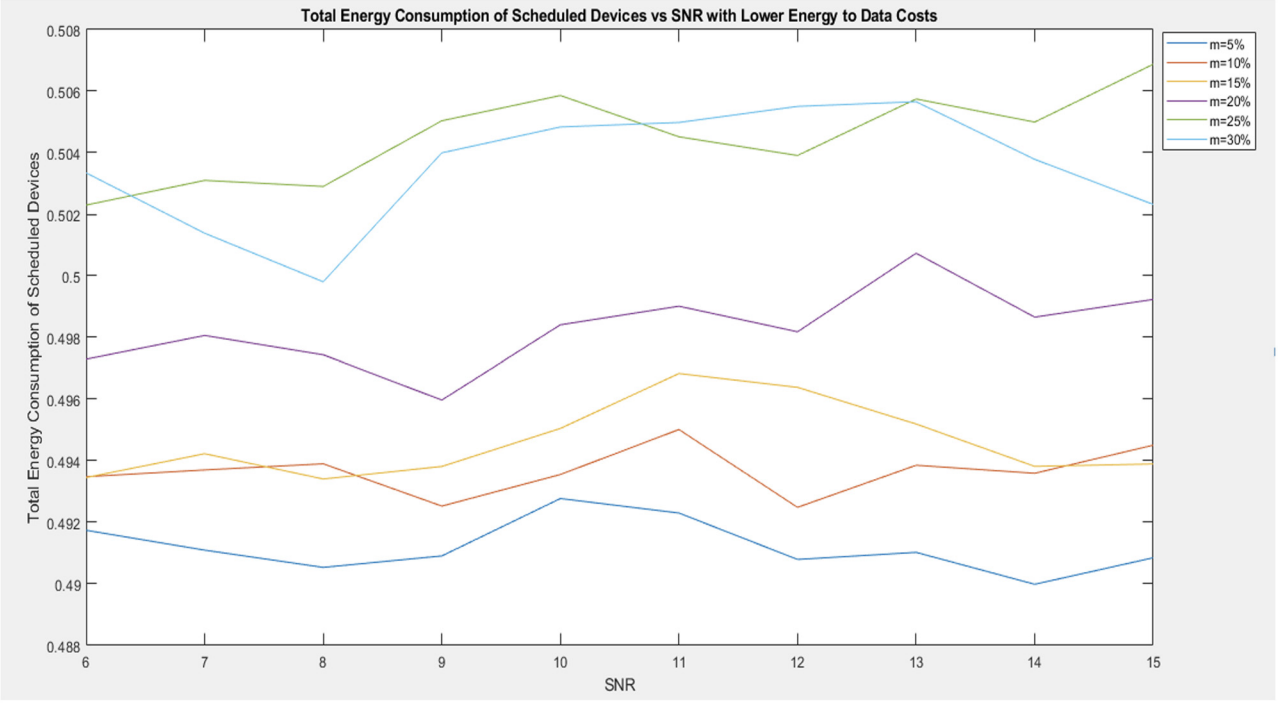


**Figure 24:** Total energy consumption of scheduled devices *vs* SNR with lower energy costs than data.

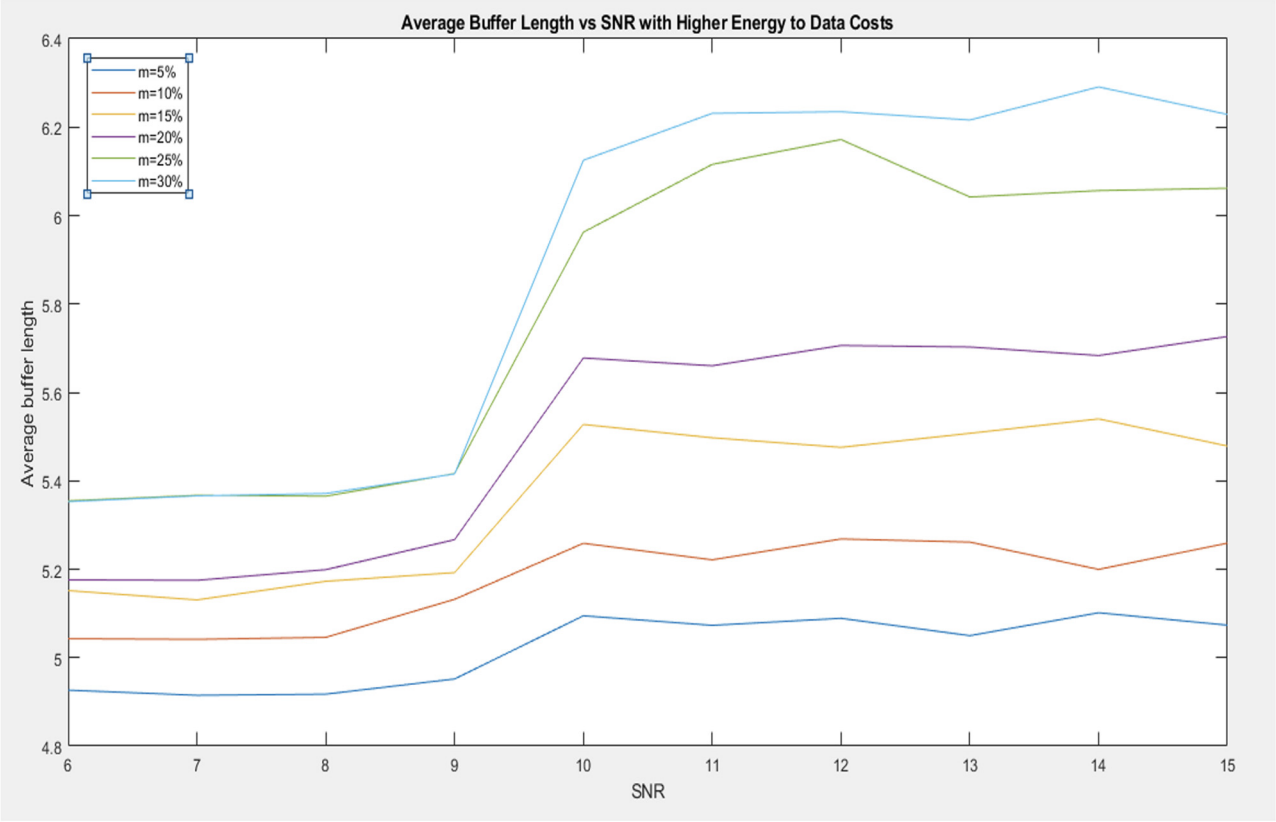


**Figure 25:** Average buffer length with higher energy costs than data.

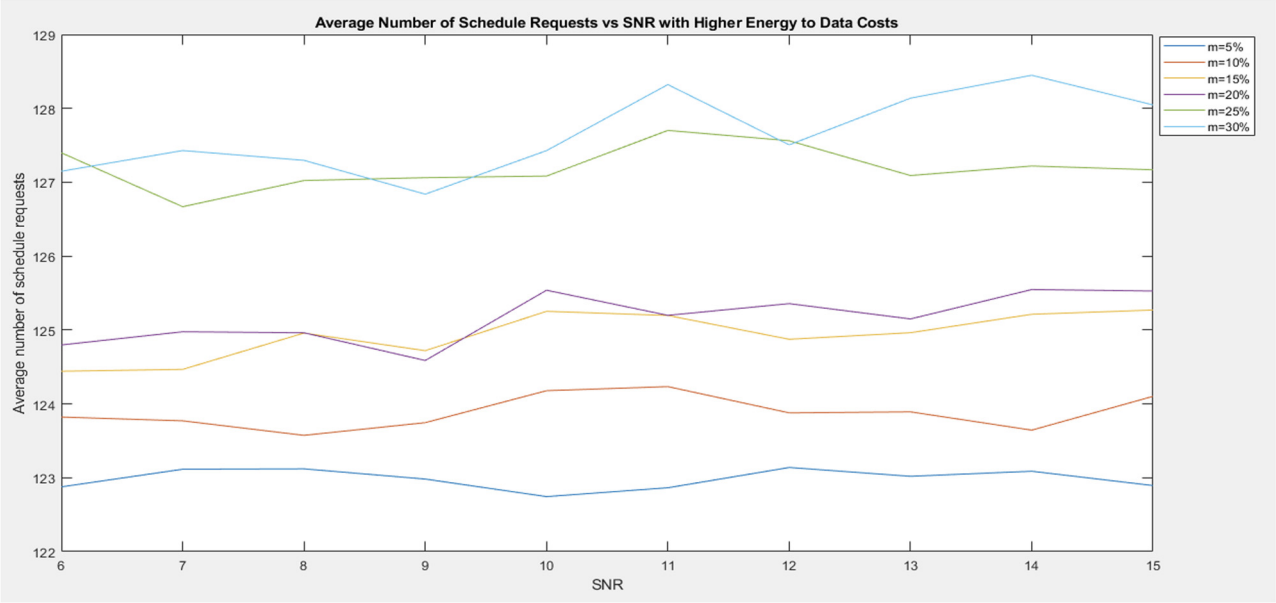


**Figure 26:** Average number of schedule requests with higher energy costs than data.

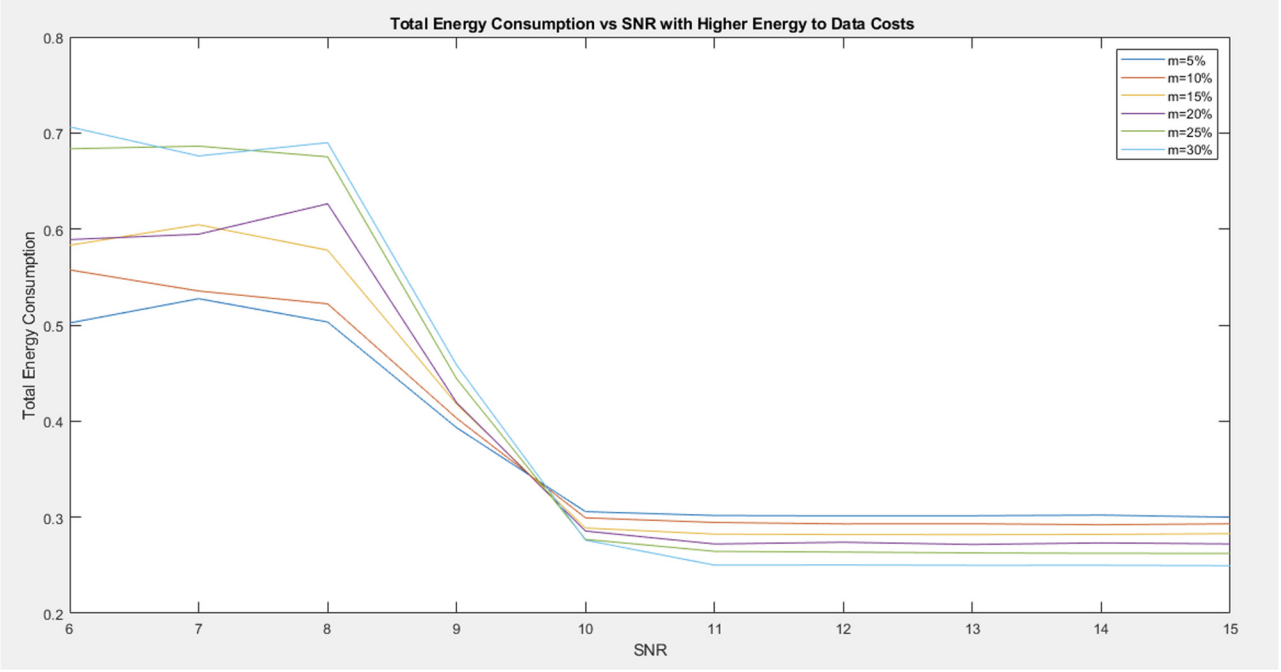


**Figure 27:** Total energy consumption *vs* SNR with higher energy costs than data.

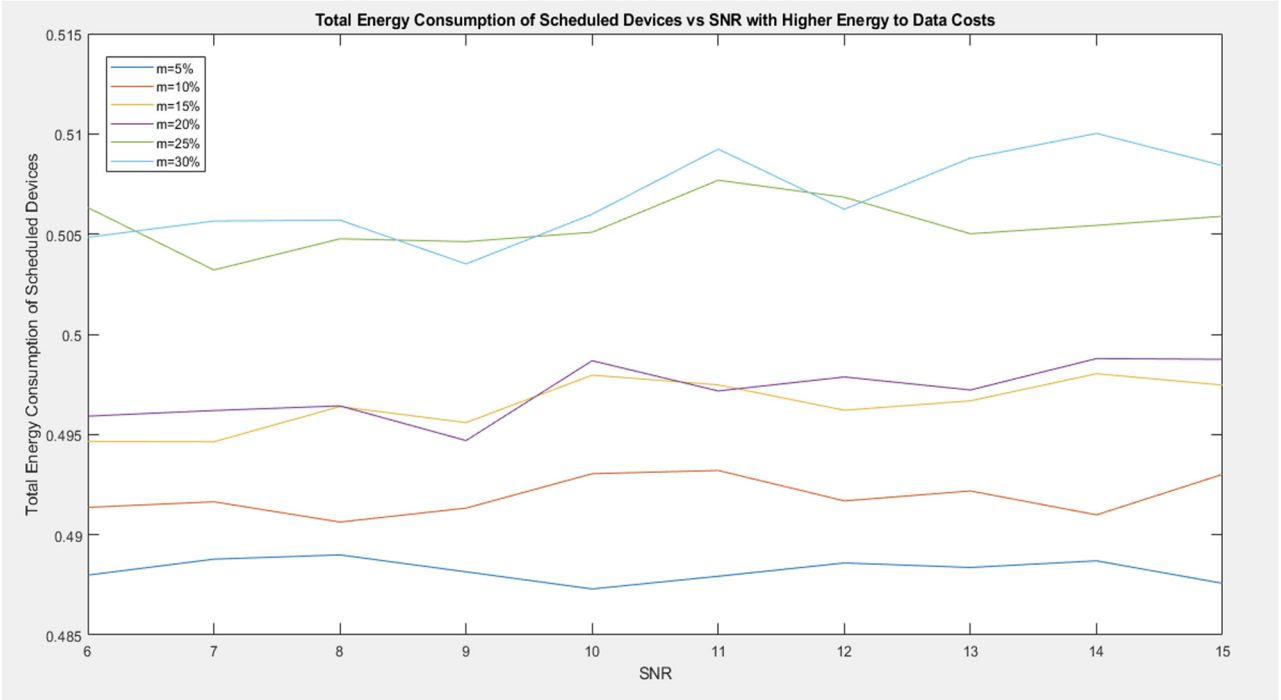


**Figure 28:** Total energy consumption of scheduled devices *vs* SNR with higher energy costs than data.

The total amount of energy used for managing and sending data is shown by the total amount of energy used when processing and storing data costs more than sending data, and there are a limited number of device transmissions at the same time (_$m$ ranging from 5 to 30%), indicated in Figure 27. A reduced number of transmitting devices requires optimized energy consumption. Through effective scheduling, the network seeks to reduce

energy usage in light of increased data processing costs. Higher SNR values result in data transport that uses less energy. In order to ensure dependable data communication while preserving energy resources in IoT networks with limited concurrent transmission capabilities, the ideal balance must be struck between energy consumption and SNR conditions, energy trade-offs, the number of devices capable of simultaneous data transmission, and memory constraints.

Figure 28 gives the total energy consumption of scheduled devices concerning SNR, while accounting for elevated energy costs for data processing compared to data transmission and limited concurrent device transmissions (_*m* from 5 to 30%), representing the energy expended for data management and transmission. With fewer devices able to transmit concurrently, efficient scheduling is crucial. High data processing costs encourage devices to schedule judiciously, especially in low SNR conditions. Finding the optimal balance involves adapting scheduling to SNR conditions, energy trade-offs, memory constraints, and the number of devices capable of simultaneous data transmission. This ensures reliable data communication while conserving energy resources in IoT networks with constrained concurrent transmission capacity.

## 4 Conclusions

The energy harvesting statistics show that the average buffer duration and the average number of planned requests rise together with the proportion of power harvesting timeslots. No matter how much energy or data costs or how many devices are used, this is true across all of the experiments. Although there is minimal difference between power harvesting when _*m* is between 15 and 20% and when it is between 25 and 30%, when we execute this in instance II, we start to witness an overlap of buffer lengths. When we look at how much energy the systems use, we can see that as the SNR rises, less energy overall is used by the devices. In every instance, we observe that all energy consumption grows as the _*m* does. This is because IoT devices use more energy in an effort to queue up data transmissions for the dwindling number of data transfer slots. In general, a timing factor of 10–20% is good for keeping the mean rate steady and boosting the system's energy efficiency. It also needs to be emphasized that the RF physics of the channel creates significant uncertainty in both the communication strength of the channel and the RF energy harvesting performed by the system. By using RF physics-based simulations of the channel, we study the variability of the system and present parameters and settings that optimize the performance of the system in such an uncertain physical state. Future work in the application of IoT networks for marine wildlife surveillance holds significant promise. Efforts should focus on the development of more advanced and energy-efficient sensors for enhanced data collection, improving real-time data processing and analysis capabilities, and the integration of artificial intelligence for species recognition and behavior monitoring. Additionally, expanding the scope to cover a broader range of marine ecosystems and species is vital. Collaboration with environmental organizations and authorities is essential to ensure the adoption and deployment of these systems for conservation and ecological research. Furthermore, addressing the environmental impact of IoT devices in marine environments and data security concerns will be critical in future endeavors.

**Funding information:** This work was funded by College of Computing, Prince of Songkla University, Phuket, Thailand.

**Author contributions:** All authors have accepted responsibility for the entire content of this manuscript and approved its submission.

**Conflict of interest:** The authors state no conflict of interest.

**Data availability statement:** All data generated or analyzed during this study are included in this published article (and its supplementary information files).

## References

[1] Abdi A, Lau WC, Alouini MS, Kaveh M. A new sim- ple model for land mobile satellite channels: first-and second- order statistics. IEEE Trans Wirel Commun. 2003;2(3):519–28.

[2] Lin D, Charbit G, Fu I-K. Uplink contention based multiple access for 5G Cellular IoT. 2015 IEEE 82nd Vehicular Technology Conference (VTC2015-Fall). Boston, MA, USA; 2015. p. 1–5. doi: 10.1109/VTCFall.2015.7391184.

[3] Huang H, Guo S, Liang W, Wang K. Online green data gathering from geo-distributed iot networks via leo satel-lites. 2018 IEEE International Conference on Communications; 2018. p. 1–6.

[4] Gharbieh M, Elsawy H, Yang HC, Bader A, Alouini MS. Spatiotemporal model for uplink iot trac:Scheduling and random-access paradox. IEEE Trans Wirel Commun. 2018;17(12):8357–72.

[5] Fraire JA, Céspedes S, Accettura N. Direct-To-Satellite IoT - A survey of the state of the art and future research perspectives. Ad-Hoc Mobile and Wireless Networks. Oct. 2019. p. 241–58.

[6] Qu Z, Zhang G, Cao H, Xie J. “LEO Satellite Constellation for Internet of Things”. IEEE Access. 2017;5:18391–401.
[7] Kodheli O, Andrenacci S, Maturo N, Chatzinotas S, Zimmer F. Resource allocation approach for differential doppler reduction in NB-IoT over LEO satellite. 2018 9th Advanced Satellite Multimedia Systems Conference and the 15th Signal Pro-cessing for Space Communications Workshop (ASMS/SPSC); Sep. 2018. p. 1–8.
[8] Jin C, He X, Ding X. “Traffic Analysis of LEO Satellite Internet of Things”. 2019 15th International Wireless Communica-tions & Mobile Computing Conference (IWCMC); Jun. 2019. p. 67–71.
[9] Pahlavan K. Understanding of RF cloud interference measurement and modeling. Int J Wireless Inf Networks. 2022;29:206–21. doi: 10.1007/s10776-021-00541-8.
[10] Alobaidy HAH, Jit Singh M, Behjati M, Nordin R, Abdullah NF. Wireless Transmissions, Propagation and Channel Modelling for IoT Technologies: Applications and Challenges. IEEE Access. 2022;10:24095–131. doi: 10.1109/ACCESS.2022.3151967.
[11] Zhang Z, Li Y, Huang C, Guo Q, Liu L, Yuen C, et al. User activity detection and channel estimation for grant-free random access in LEO satellite-enabled in-ternet of things. IEEE Internet Things J. 2020 Sep;7(9):8811–25.
[12] Viswanathan H, Mogensen PE. Communications in the 6G Era. IEEE Access. 2020;8:57063–74.
[13] Soussi ME, Zand P, Pasveer F, Dolmans G. Evaluating The performance of emtc and nb-iot for smart city applica-tions. 2018 IEEE International Conference on Communications (ICC); 2018. p. 1–7.
[14] Wang W, Tong Y, Li L, Lu AA, You L, Gao X. Near op- timal timing and frequency offset estimation for 5g inte-grated leo satellite communication system. IEEE Access. 2019;7(1):113–298.
[15] Van Kranenburg R. The Internet of Things: A critique of ambient technology and the all-seeing network of Rfid. Amsterdam, The Netherlands: Institute of Network Cultures; 2008.
[16] Konde S, Deosarkar DS. IOT Based Water Quality Monitoring System. 2nd International Conference on Communication & Information Processing (ICCIP) 2020; June 4, 2020. https://ssrn.com/abstract=3645467. doi: 10.2139/ssrn.3645467.
[17] Maraveas C, Asteris PG, Arvanitis KG, Bartzanas T, Loukatos D. Application of bio and nature-inspired algorithms in agricultural engineering. Arch Computat Methods Eng. 2023;30:1979–2012. doi: 10.1007/s11831-022-09857-x.
[18] Maraveas C, Piromalis D, Arvanitis KG, Bartzanas T, Loukatos D. Applications of IoT for optimized greenhouse envi-ronment and resources management. Comput Electron Agric. 2022;198:106993. doi: 10.1016/j.compag.2022.106993.
[19] Xu G, Shi Y, Sun X, Shen W. Internet of things in marine environment monitoring: A review. Sensors. 2019;19(7):1711. doi: 10.3390/s19071711.
[20] Lakshmikantha V, Hiriyannagowda A, Manjunath A, Patted A, Basavaiah J, Anthony AA. IoT based smart water quality monitoring system”. Glob Transit Proc. 2021;2:181–6.
[21] Pasika S, Gandla ST. Smart water quality monitoring system with cost-effective using IoT. Heliyon. 2020;6:e04096.
[22] Mariani P. Collaborative automation and IoT technologies for coastal ocean observing systems. Front Mar Sci Sec Ocean Observation. 2021 Aug;8:1–8. doi: 10.3389/fmars.2021.647368.
[23] Tiwari R, Rachmawati UA, Pandey B. Iot based monitoring for sustaining life be-low water and protecting our marine economy. Eur Chem Bull. 2023;12(S3):6571–80.
[24] Bharati S, Podder P. Machine and deep learning for IoT security and privacy: Applications, challenges, and future directions. Hindawi Secur Commun Netw. 2022;2022:1–41. Article ID 8951961 doi: 10.1155/2022/8951961.
[25] Petrovic R, Simic D, Cica Z, Drajic D, Nerandzic M, Nikolic D. IoT OTH maritime surveillance service over satellite net-work in equatorial environment: Analysis, Design and deployment. Electronics. 2021;10(17):2070. doi: 10.3390/electronics10172070.
[26] Sugapriyaa T, Rakshaya S, Ramyadevi K, Ramya M, Rashmi Smart PG. water quality monitoring system for real time applications. Int J Pure Appl Math. 2018;118:1363–9.
[27] Yang C, Shen W, Wang X. Internet of Things in manufacturing: An overview. IEEE SMC Mag. 2018;4:6–15.
[28] Cook DJ, Crandall AS, Thomas BL, Krishnan NC. Casas: A smart home in a box. Computer. 2013;46:62–9.
[29] Komninos N, Philippou E, Pitsillides A. Survey in smart grid and smart home security: Issues, challenges and counter-measures. IEEE Commun Surv Tutor. 2014;16:1933–54.
[30] Talcott C. Cyber-physical systems and events. In: Software-Intensive Systems and New Computing Paradigms. Berlin/Heidelberg, Germany: Springer; 2008. p. 101–15.
[31] Yongfu L, Dihua S, Weining L, Xuebo Z. A service-oriented architecture for the transportation cyber-physical systems. In: Proceedings of the 31st Control Conference (CCC). Hefei, China: 25–27 July 2012. p. 7674–8.
[32] Ungurean I, Gaitan N-C, Gaitan VG. An IoT architecture for things from industrial environment. Proceedings of the 10th International Conference on Communications (COMM). Bucharest, Romania; 29–31 May 2014. p. 1–4.